AD NUMBER

AD905720

LIMITATION CHANGES

TO:

Approved for public release; distribution is unlimited.

FROM:

Distribution authorized to U.S. Gov't. agencies only; Test and Evaluation; NOV 1972. Other requests shall be referred to Naval Civil Engineering Laboratory, Port Hueneme, CA 93043.

AUTHORITY

USNCBC ltr dtd 24 Oct 1974

Technical Report

R 780

Sponsored by

PICATINNY ARSENAL

November 1972

NAVAL CIVIL ENGINEERING LABORATORY

Port Hueneme, California 93043

DETERMINATION OF BLAST LEAKAGE PRESSURES AND FRAGMENT VELOCITY FOR FULLY VENTED AND PARTIALLY VENTED PROTECTIVE CUBICLES

DETERMINATION OF BLAST LEAKAGE PRESSURES AND FRAGMENT VELOCITY FOR FULLY VENTED AND PARTIALLY VENTED PROTECTIVE CUBICLES

Technical Report R-780

51-031

by

J. M. Ferritto

ABSTRACT

Blast leakage pressures acting on a structure surrounding a protective cubicle were experimentally determined in a one-third scale model test. Nineteen pressure transducers were used to record the blast environment within the cubicle and on the surrounding structure. Variations in venting area were tested. Results indicate that the pressures can be sufficiently high to cause damage to conventional construction; however, the pressures can be reduced to safe levels by restricting the venting. The velocity of secondary fragments produced from the breakup of simulated processing equipment subjected to the blast of full-size 81-mm mortars was determined. Photographic coverage and calculation of fragment penetration in backstops indicate heavy secondary fragments are capable of traveling considerable distances at relatively high velocities.

CONTENTS

FOREWORD

This research was performed at the Naval Civil Engineering Laboratory under work unit number 51-031. Inclusive dates of research were November 1971 to March 1972. The report was submitted in June 1972 by the Project Engineer, Mr. John Ferritto.

Funding and overall supervision of this project was provided by Picatinny Arsenal as part of their program to establish safety design criteria for storage and processing of explosives. This test effort was part of the engineering assistance Picatinny Arsenal provides to MUCOM facilities. Mr. Richard Rindner, Picatinny Arsenal, was program manager and administered this test program. Mr. Norval Dobbs, Ammann and Whitney, as part of a contract with Picatinny Arsenal provided consultation and assistance in the test program requirements.

INTRODUCTION

Background

A modernization program is being conducted by the U. S. Army Munitions Command to upgrade explosive production facilities used in the manufacture of conventional ammunition. Several of the operations to be performed in the new facilities are considered hazardous and special provisions must be made to protect operating personnel in areas adjoining the hazardous operating stations. A concept has been proposed that would utilize a protective cell in which the blast effects from an accidental internal explosion would be vented through a frangible roof. The protective cell must be capable of resisting the initial blast of the explosion. However, this approach eliminates the requirement that the protective cell be capable of providing full confinement of the blast and resisting the longer duration gas accumulation pressures. The frangible roof allows the vented pressures to leak out of the top of the protective cell onto the exterior of the surrounding structure. The magnitudes of the leakage pressures were unknown and required investigation to determine whether they were high enough to produce structural damage to the surrounding building and injure personnel. The Naval Civil Engineering Laboratory (NCEL) has been tasked to conduct this investigation.

Objective

The objective of this test program was to experimentally determine the blast leakage pressures acting on a structure surrounding a protective cubicle and to determine the velocity of secondary fragments caused by the breakup of processing equipment. The test program included:

1. Determination of the blast environment within fully vented and partially vented protective cubicles.
2. Determination of the blast pressures on the adjacent structure.
3. Determination of the velocity of secondary fragments produced by the breakup of processing equipment.

Theory

When an explosion occurs within a protective cubicle, the pressure can be extremely high and will be amplified by reflections off the cubicle walls and floor. The accumulation of gases from the explosion will exert additional pressure and increase the load duration; unless the cubicle is designed to contain the total pressure, venting of the gas and shock pressure must be provided. The buildup of the gas pressure is dependent upon the weight of the charge, the volume of the confining structure, and the size of the vents.

For a protective cubicle with full venting, the resulting blast wave on the exterior of the surrounding structure will be appreciably modified compared with that of an unbarricaded detonation. As the blast wave propagates outward, the shock front strikes the interior surfaces, which reinforce the initial pressure and impulse. The shock pressure will eventually spill over the structure. Initially, the exterior pressure will not have a definite shock front; however, a shock front will develop at some distance from the structure. Tests have been performed on a concrete cubicle in which the roof and one wall were open.* Predicted pressure levels were determined from analysis of the test results.

BLAST ENVIRONMENT—FULLY VENTED CUBICLE

Approach

The determination of the blast environment in the cubicle and on the surrounding structure has been divided in five parts simulating the effects of:

1. The simultaneous detonation of two 81-mm projectiles.
2. The simultaneous detonation of six 81-mm projectiles.
3. The simultaneous detonation of ten 81-mm projectiles.
4. The nonsimultaneous detonation of six 81-mm projectiles.
5. The detonation of heavier charges.

---

* Naval Facilities Engineering Command. NAVFAC P-397: Structures to resist the effects of accidental explosion. Washington, D. C., June 1969. (Also Army TM-5-1300; AFM-88-22.)

The tests were conducted on a one-third scale model. By use of geometric scaling laws, all dimensions of the test structure were reduced to one-third those of the full-scale structure. The explosive charge was 1/27 the weight of the actual explosive contained in the 81-mm projectile. Pressures were measured within the cubicle and along the roof of the structure.

Test Procedure

Structure. A protective cell consisting of four walls and a floor was fabricated from 3-inch steel plate. Soil was placed around the cell forming the outline of the surrounding structure. The soil was held in place by retaining walls and covered with plywood sheets. Figures 1 through 5 show the test structure. Gage mounts were located in the protective cell and along the roof of the surrounding structure.

Explosive Charges. Two 81-mm projectiles to be exploded simultaneously were represented by a 0.19-pound cylinder of composition B explosive, six projectiles by a 0.50-pound cylinder of compositon B, and ten 81-mm projectiles by a 0.93-pound cylinder of composition B. The cylinders were cast and machined to within 1% of exact weight. The cylinder aspect ratio (diameter to height) was 1.0 (Figure 6).

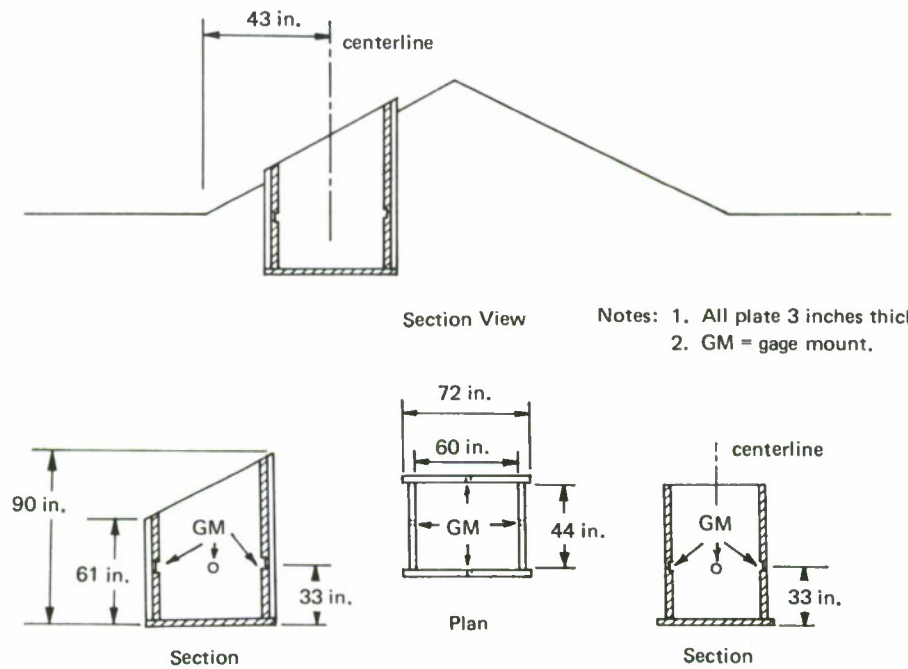

Figure 1. Details of test structure cubicle.

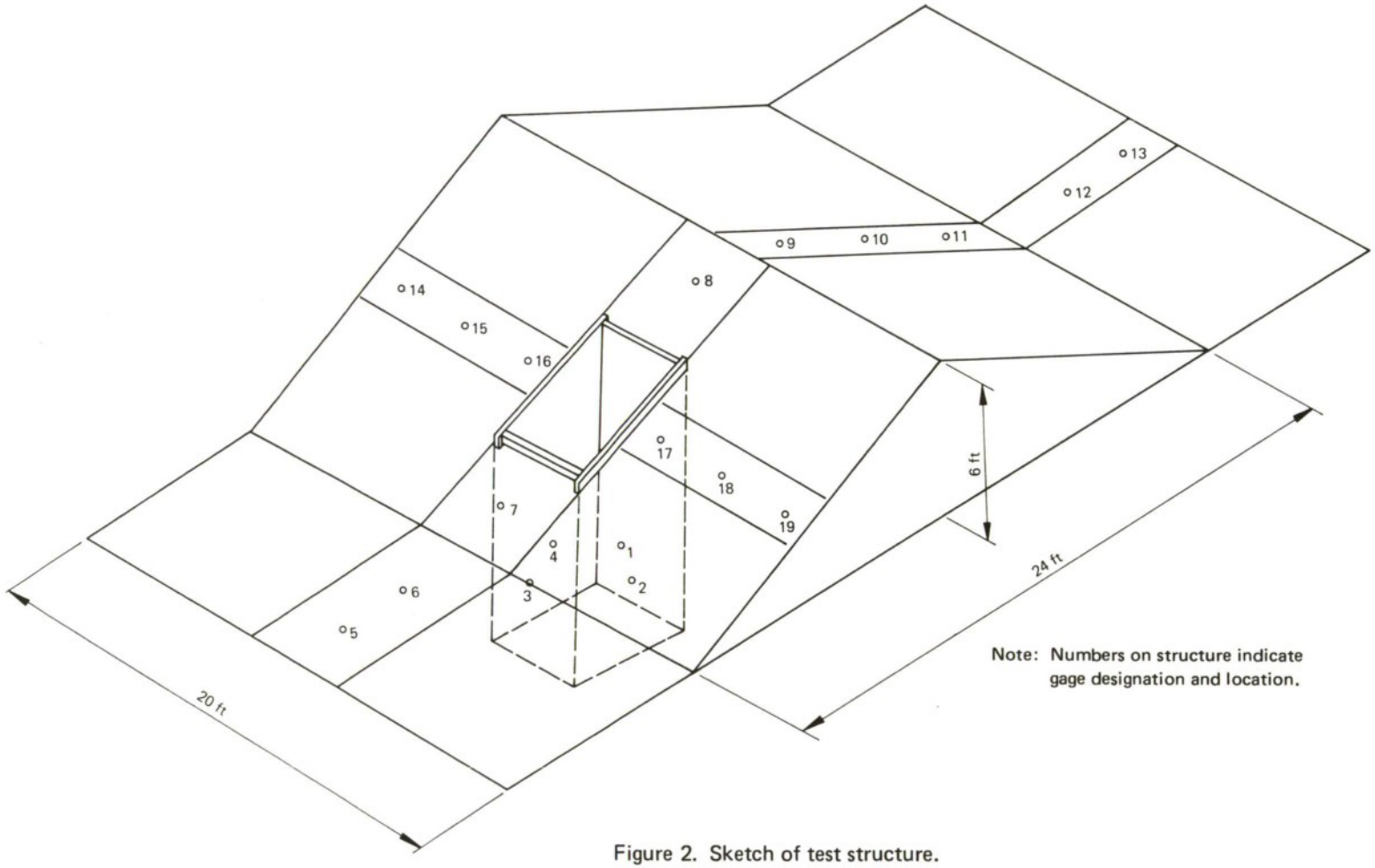

Figure 2. Sketch of test structure.

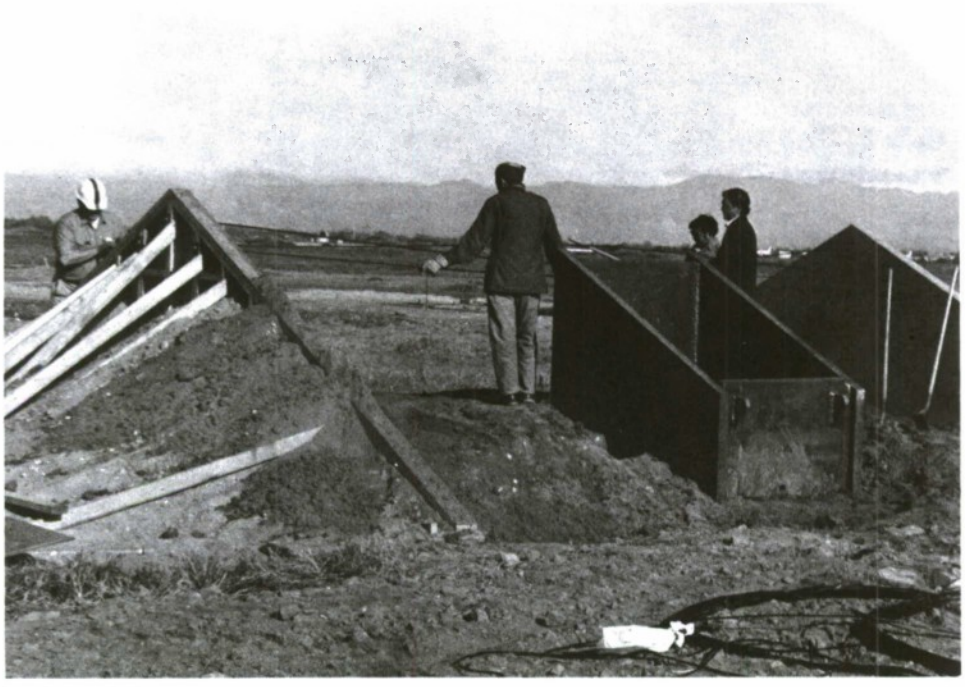

Figure 3. Test structure under construction.

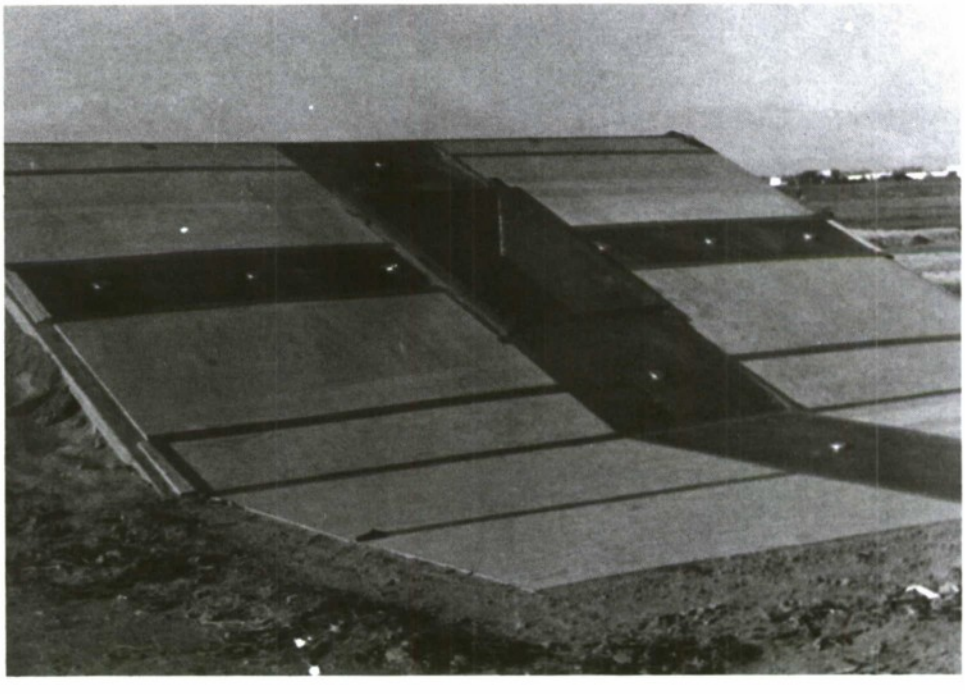

Figure 4. Front view of test structure, showing cubicle and gage line.

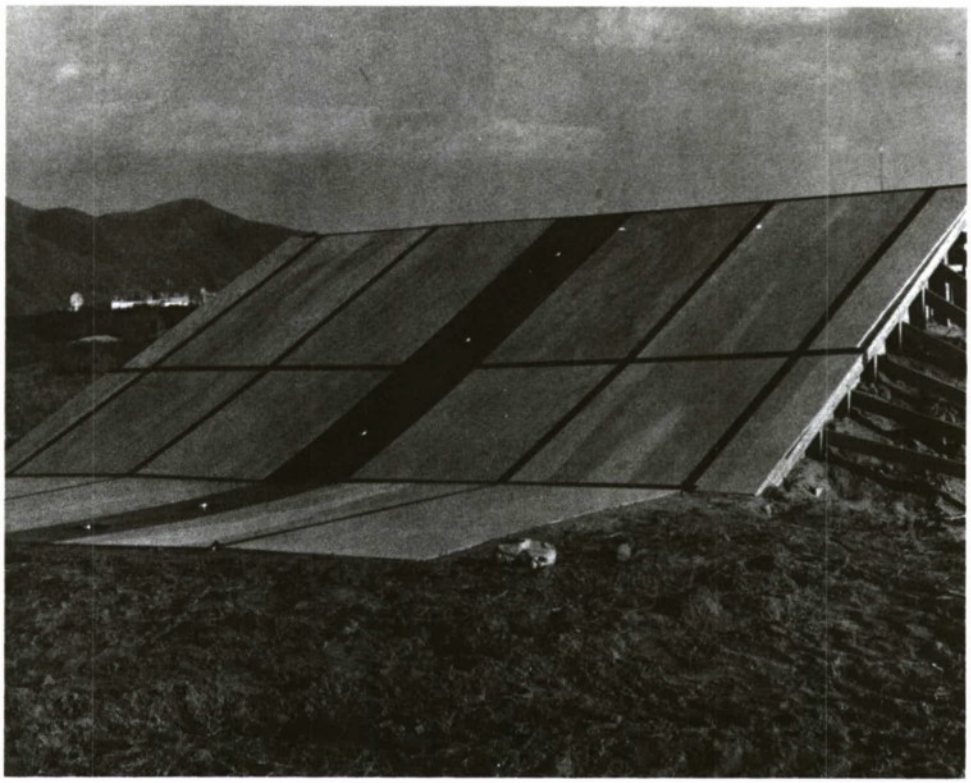

Figure 5. Rear view of test structure, showing gage line.

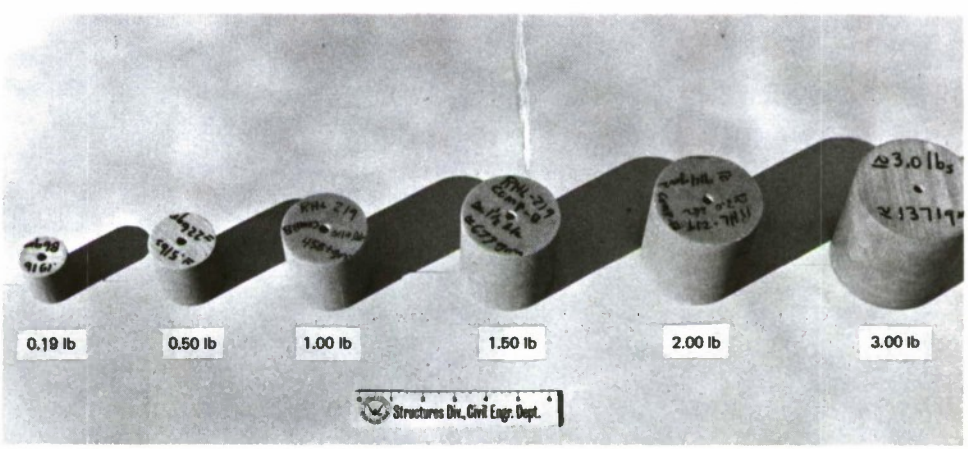

Figure 6. Composition B explosive charges.

Instrumentation

Nineteen pressure transducers were used to measure the intensity of the blast environment, four within the cell and 15 on two gage lines on the roof (Figure 7). The four transducers within the cell were located in the center of the width of each wall and 30 inches above the floor.

The Bytrex pressure transducers are specifically designed to measure blast phenomena. They are acceleration resistant, mechanically rugged, and equipped with a heat shield to reduce the effects of thermal radiation. They incorporate semiconductor sensing elements that produce a high electrical output minimizing system electrical noise. The gages were directly calibrated in place by static pressurization.

The recording system for the close-in gages included Endevco 4401 signal conditioners, Dana 3850 V2 amplifiers, and a Sangamo Saber 4 tape recorder. The recorder was operated at 120 ips and the system was capable of flat response to 30 kHz.

The recording system for the remaining gages included Endevco 4470 signal conditioners, modules with Endevco 4472.6 amplifiers, and a Sangamo 3564 tape recorder. The recorder was operated at 60 ips and the system was capable of flat response to 20 kHz. A Systron-Donner 8150 time code generator provided IRIG-B timing. A program sequencer was used to control the system and detonate the charge.

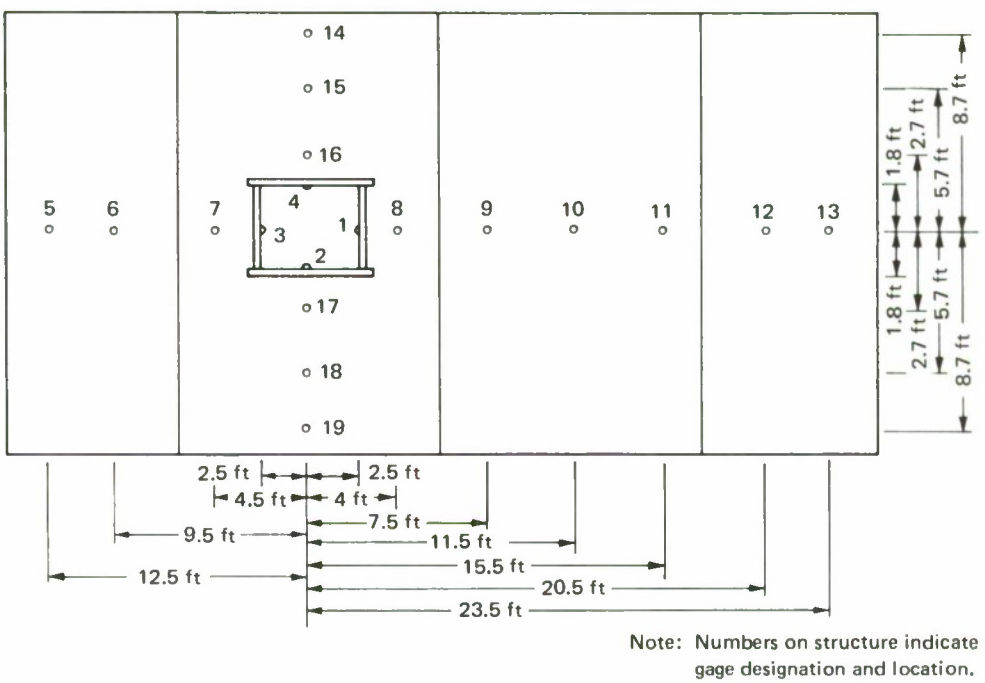

Note: Numbers on structure indicate gage designation and location.

Figure 7. Plan view of structure, showing instrumentation position.

Data were digitized with an FR 1400 tape recorder, EMR 4143 proportional bandwidth discriminators, an Electronic Engineering Company high-speed digitizer, and a Wyle Laboratories digital spectrum analyzer system. The analog data were digitized and recorded on magnetic tape. The digitized data tape was read by the digital spectrum analyzer system, which integrated the data, producing the impulse profiles and the peak values. Digitized data of the pressure and impulse were plotted with an IBM 7094 computer and SC 4020 plotters.

Data Accuracy

Recording System. The data recording equipment had the following specifications on accuracy:

Pressure transducer linearity and hysteresis	2%
Signal conditioner and amplifier linearity and gain	1.5%
Tape recorder wow and flutter	1%
Tape recorder linearity and gain	0.5%

Each channel was individually calibrated by applying a static pressure equal to the predicted pressure value. The maximum deviation between the recorded pressure and the actual pressure is 3%. The deviation between equivalent tests is 1%.

Data Reduction System. The data reduction equipment had the following specifications on accuracy:

Tape recorder tape speed	0.2%
Tape recorder harmonic distortion	<3%
Proportional bandwidth discriminator center frequency	1%
Proportional bandwidth discriminator zero stability drift	0.5%
Proportional bandwidth discriminator harmonic distortion	<1%
High-speed digitizer	0.5%

Data were sampled at the rate of 160 samples per msec. The maximum deviation between the digitized data and the actual recorded data was less than 2%.

The maximum deviation between the digitized data and the actual pressure data was less than 5%, with an average deviation of 3.6%.

Results of Blast Tests

The following tests were conducted:

Number of Shots	Charge Weight (lb)
5	0.19
5	0.50
5	0.93
5	3 each of 0.19
3	2.00
3	3.00

All of the preceding tests were conducted with the charges centered in the cubicle, 12 inches above the cubicle floor. In the case of the three 0.19-pound charges, one charge was centered in the cubicle 12 inches above the cubicle floor and the other two charges were located at the same elevation 7 inches on either side parallel to the narrow sides of the cubicle. The three charges were fired simultaneously by three blasting caps wired in series.

The peak pressures observed for the various charge weights are summarized in Table 1 and plotted in Figures 8 and 9. Peak positive impulses are summarized in Table 2. Figure 10 gives typical pressure and impulse curves for the various gages for a charge weight of 0.50 pound. Figure 11 gives the internal cubicle pressure for various charge weights. The geometry of the cubicle, the location of the gages relative to the location of the charge, and the angle of incidence all affect the reflection factor and the clearing time and thus affect the pressure histories.

It was of interest to investigate the effect of variation of charge height on pressure distribution. One-pound charges were fired with the charges centered in the cubicle, 30 inches above the cubicle floor and also at 44 inches above the cubicle floor. The peak pressures from these tests are given in Table 3 and plotted in Figures 12 and 13. Peak positive impulses are given in Table 4.

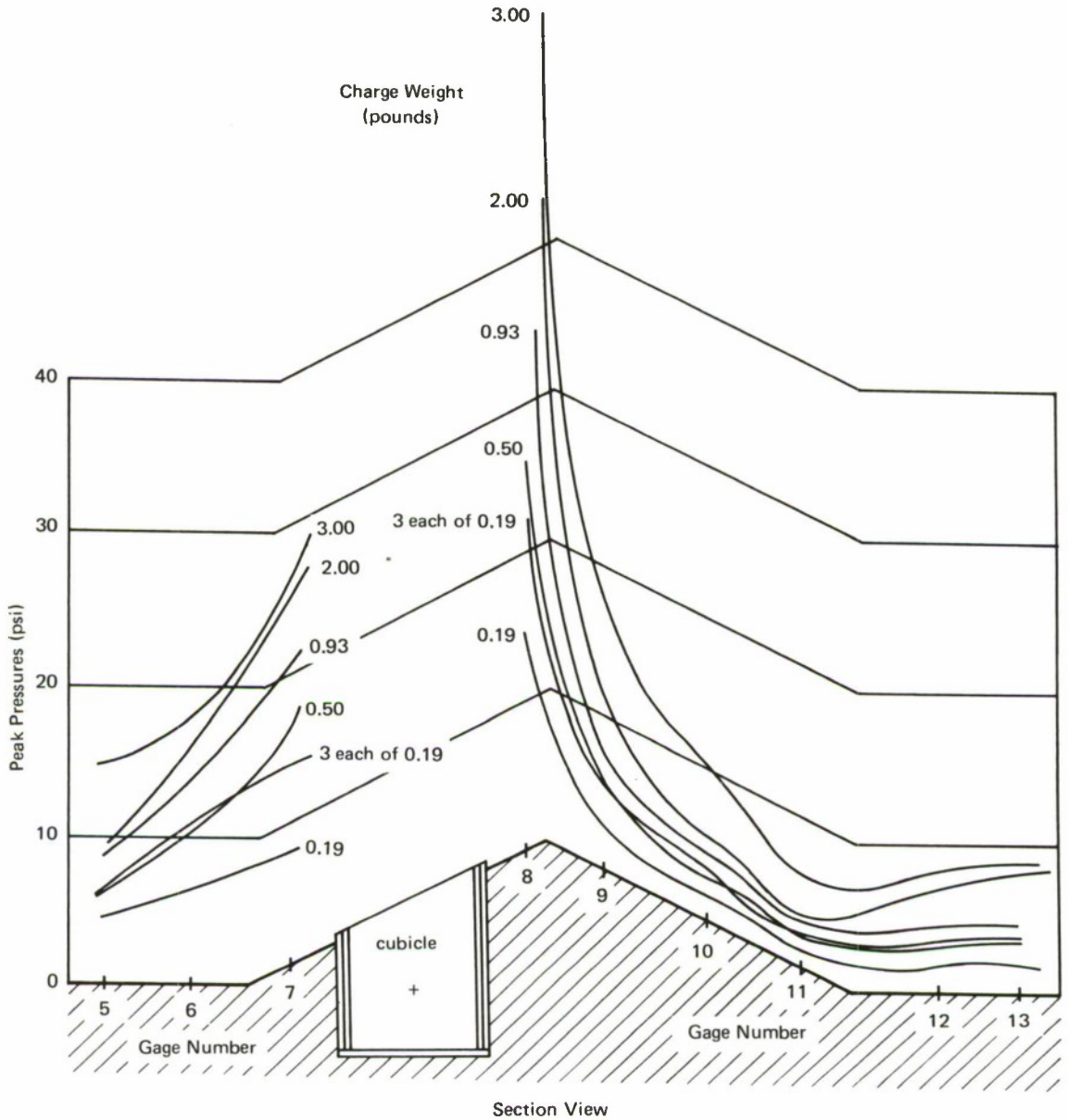

Figure 8. Peak pressures for various charge weights (gages 5 through 13).

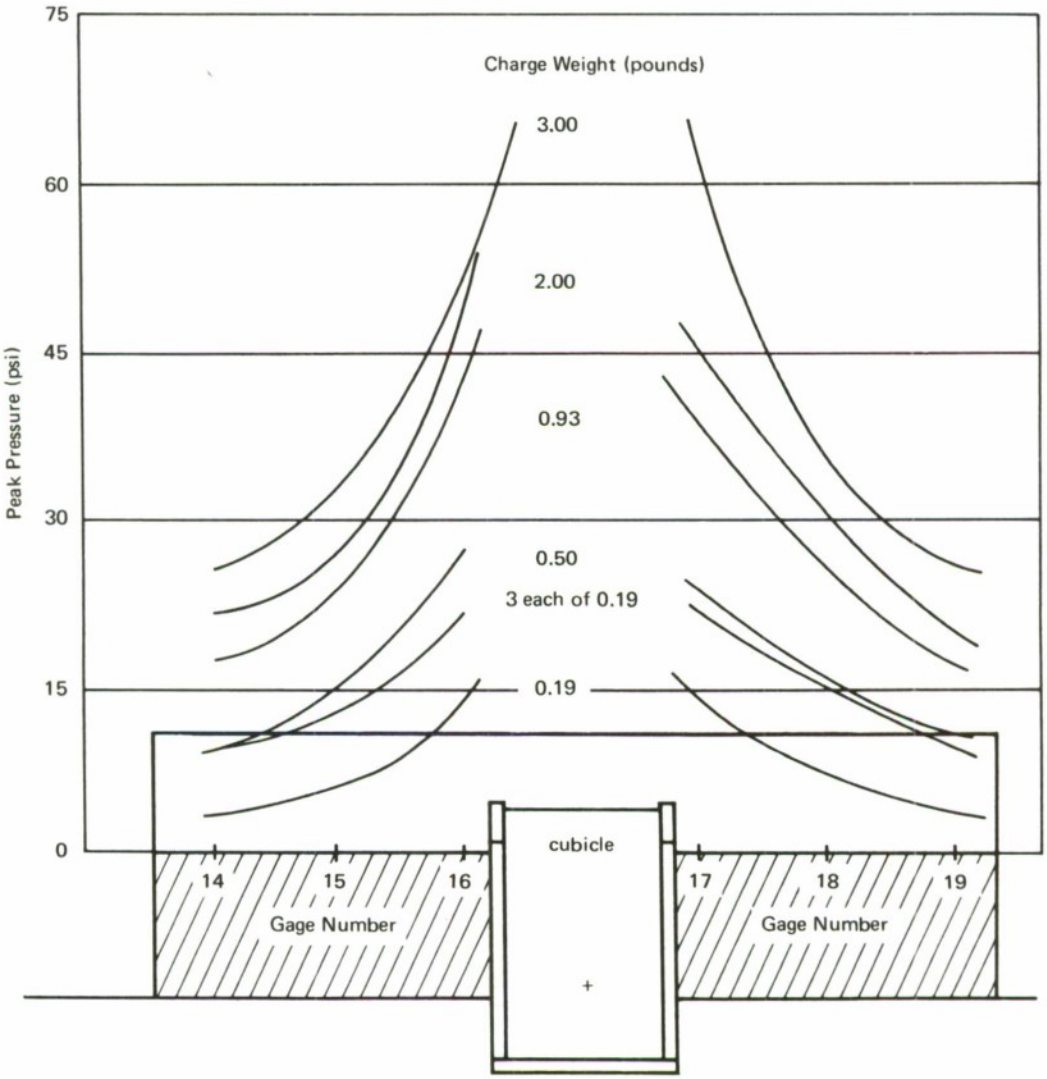

Figure 9. Peak pressures for various charge weights (gages 14 through 19).

Table 1. Peak Pressures for Various Charge Weights

Gage	Peak Pressures (psi) for Charge Weights (lb) of—					
	0.19	3 each of 0.19	0.50	0.93	2.00	3.00
1	98.9	310.8	142.7	242.0	435.0	652.2
2	133.6	331.3	205.2	268.2	381.7	585.7
3	127.9	215.5	157.7	231.7	527.1	603.1
4	113.0	253.2	215.8	273.7	449.3	593.6
5	4.79	6.54	6.49	8.83	10.07	15.39
6	6.76	11.00	10.63	14.79	16.63	17.84
7	7.56	13.21	16.48	20.51	25.66	26.15
8	14.21	21.47	23.96	34.40	43.81	58.75
9	2.48	5.93	5.47	7.67	12.14	16.56
10	1.34	3.25	2.80	4.38	5.62	10.19
11	1.02	1.70	1.56	2.79	3.63	5.29
12	1.75	3.52	3.37	4.38	7.24	8.18
13	1.68	3.60	3.54	4.58	7.80	8.53
14	3.59	9.16	9.28	16.90	21.08	25.63
15	5.55	12.71	14.32	23.70	27.15	31.83
16	13.80	21.10	27.61	43.10	50.71	51.00
17	13.58	21.34	23.51	37.20	44.60	63.48
18	6.66	14.82	16.43	25.54	30.28	34.34
19	3.47	9.45	10.48	16.28	19.49	25.48

Table 2. Peak Total Positive Impulses for Various Charge Weights

Gage	Peak Impulses (psi-msec) for Charge Weights (lb) of—					
	0.19	3 each of 0.19	0.50	0.93	2.00	3.00
1	81.7	136.6	142.0	192.4	238.6	296.6
2	78.5	138.4	122.3	154.5	201.5	241.9
3	62.5	138.9	111.8	197.8	276.4	657.2
4	109.4	172.2	159.1	217.8	366.6	566.3
5	3.17	5.81	5.37	7.70	10.34	12.99
6	3.28	7.28	7.43	10.66	13.19	17.10
7	3.68	5.54	5.66	7.90	10.40	16.72
8	6.94	10.22	10.88	14.33	17.07	23.24
9	2.57	4.70	4.14	5.73	8.28	9.98
10	1.51	3.27	2.79	3.89	6.12	7.24
11	1.25	2.99	2.43	3.46	5.56	6.80
12	1.13	2.55	2.21	3.10	4.96	6.18
13	0.98	2.37	1.97	2.78	4.53	5.65
14	4.05	8.91	7.95	10.49	15.29	18.46
15	5.23	10.06	8.98	11.68	15.39	17.79
16	5.74	5.33	10.58	14.85	13.64	18.58
17	6.30	5.98	10.10	16.53	16.74	24.23
18	5.66	11.11	9.29	12.56	16.83	20.49
19	3.91	8.04	6.59	10.37	12.56	15.86

Note: Average of 5 tests.

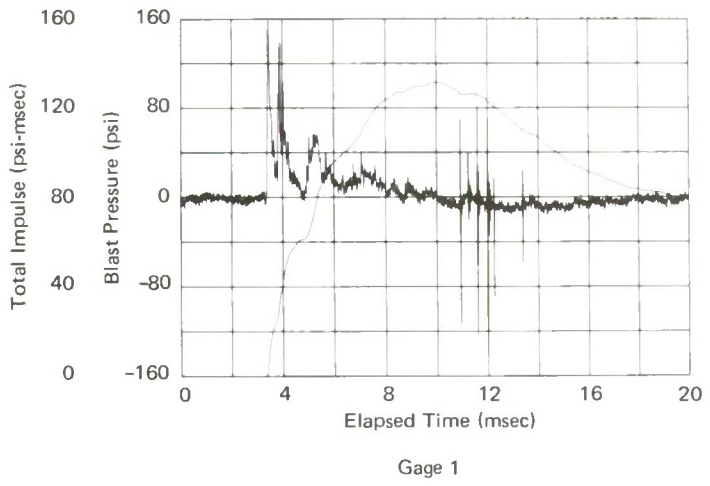

Gage 1

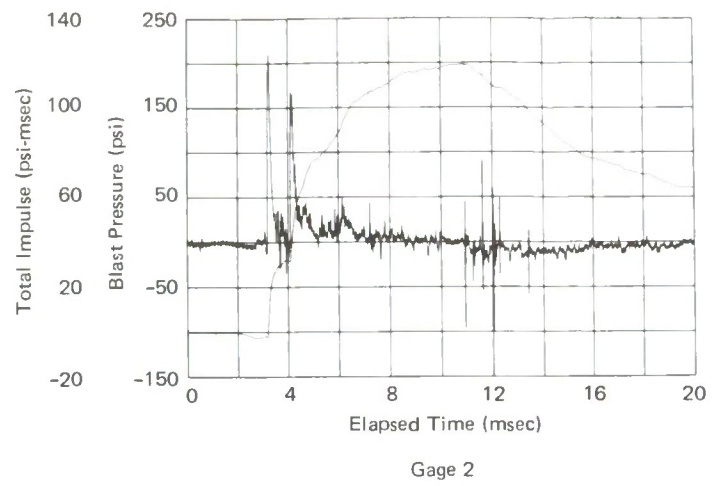

Gage 2

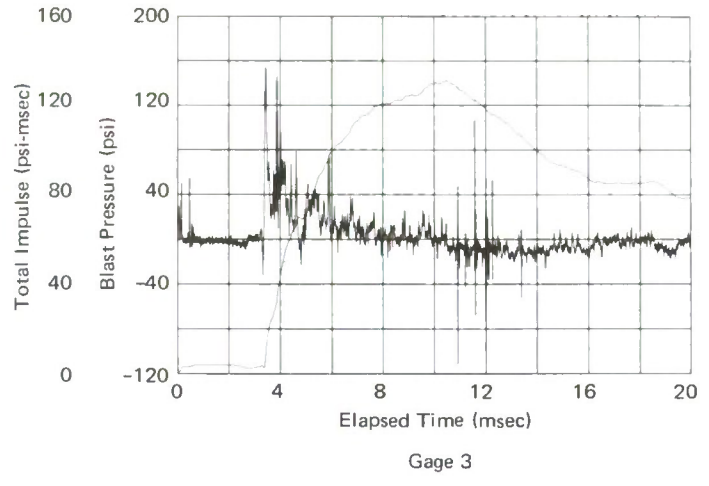

Gage 3

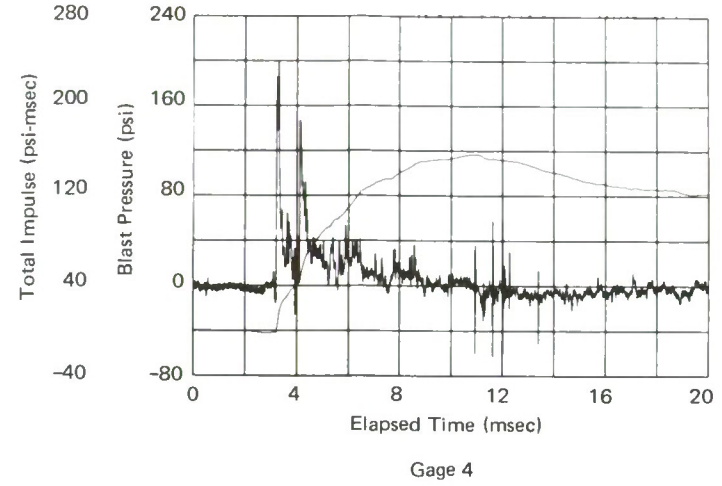

Gage 4

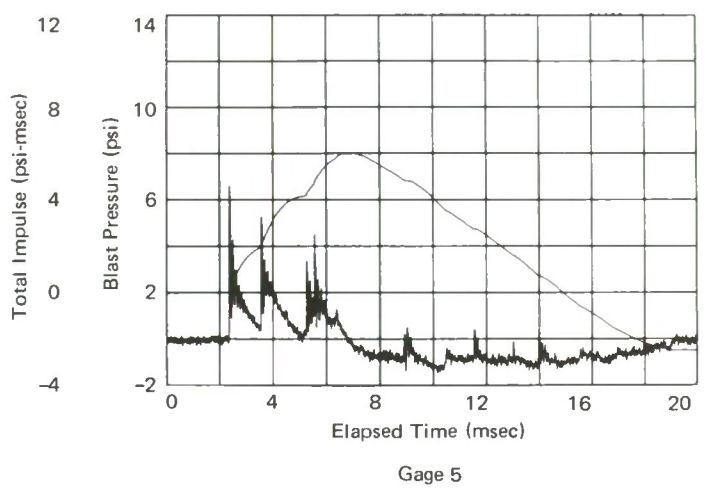

Gage 5

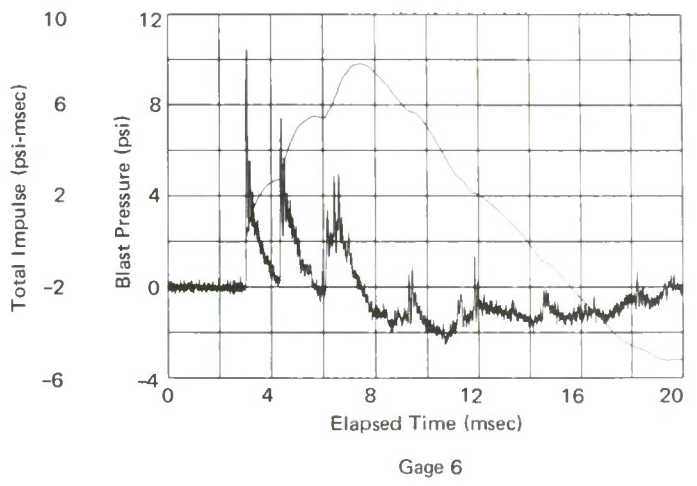

Gage 6

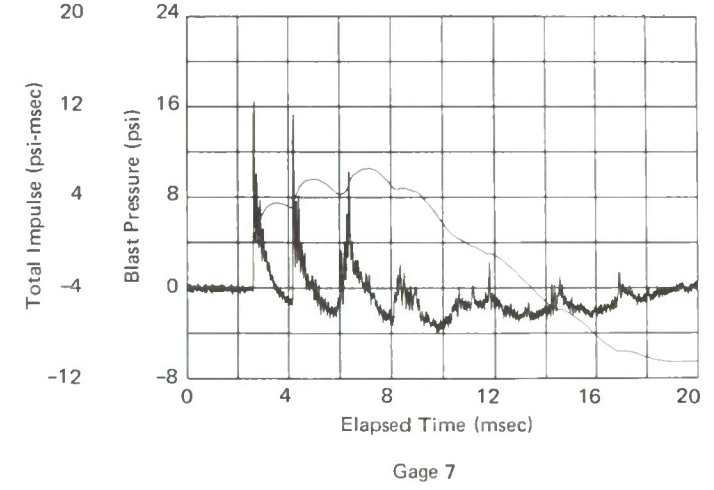

Gage 7

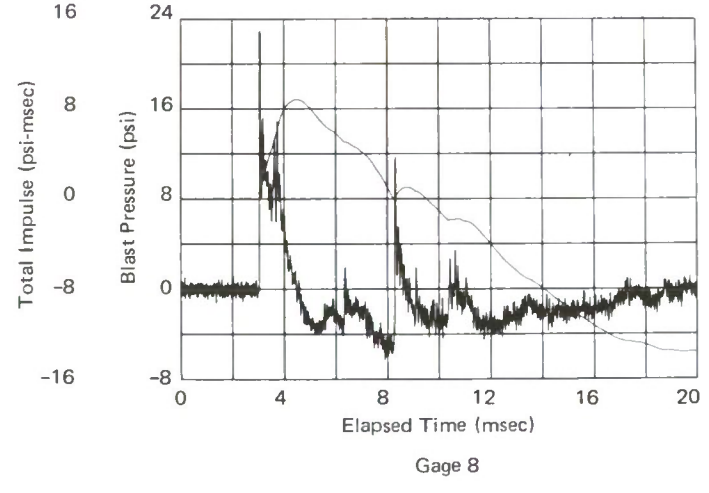

Gage 8

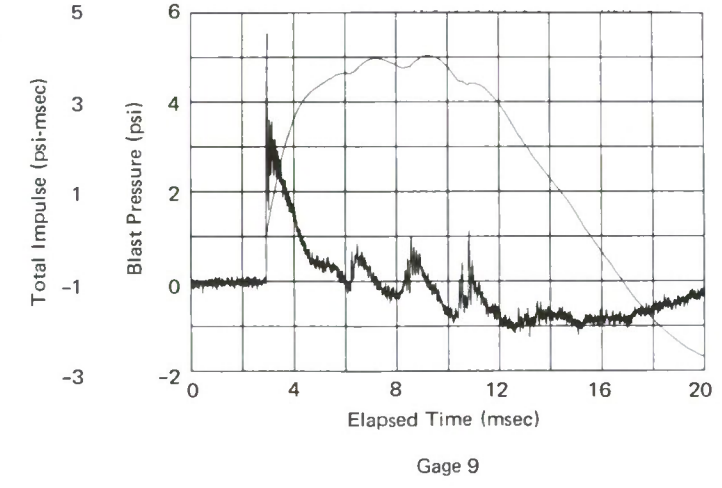

Gage 9

Test 323
Charge: 0.50 lb
Temperature: 57°F
Barometric Pressure: 30.016 in. Hg
Wind: 8 knots from 270 deg
Cover: clear

Figure 10. Typical pressure and impulse data.

Continued

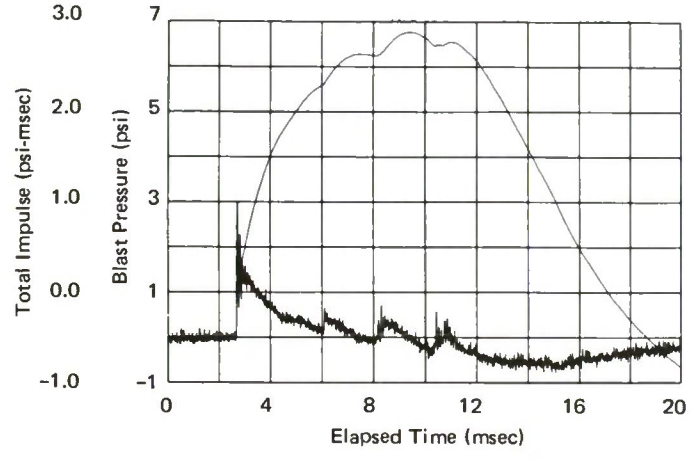

Gage 10

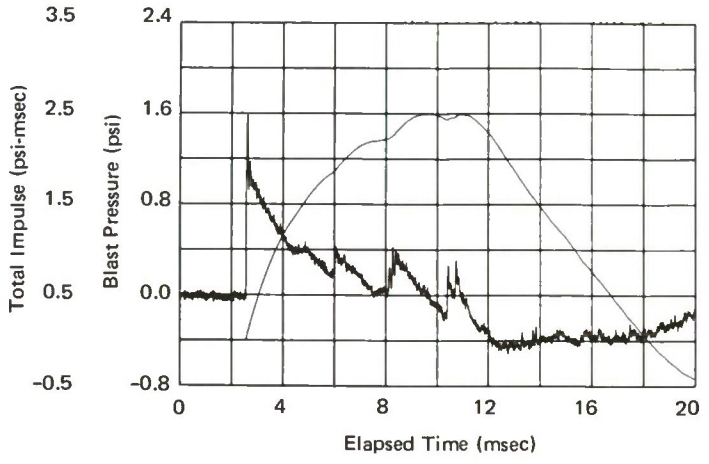

Gage 11

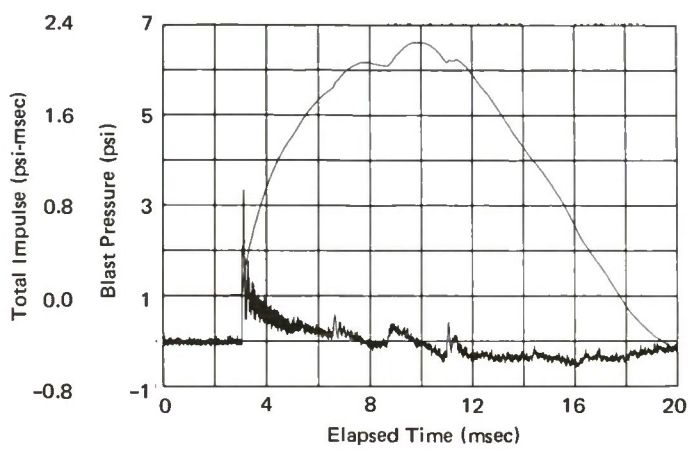

Gage 12

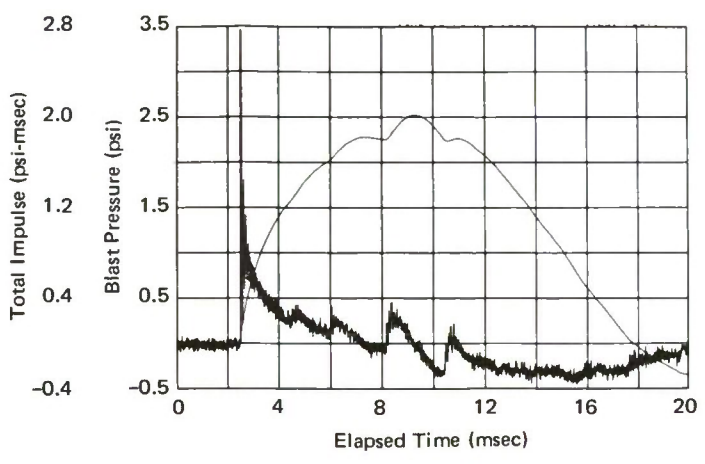

Gage 13

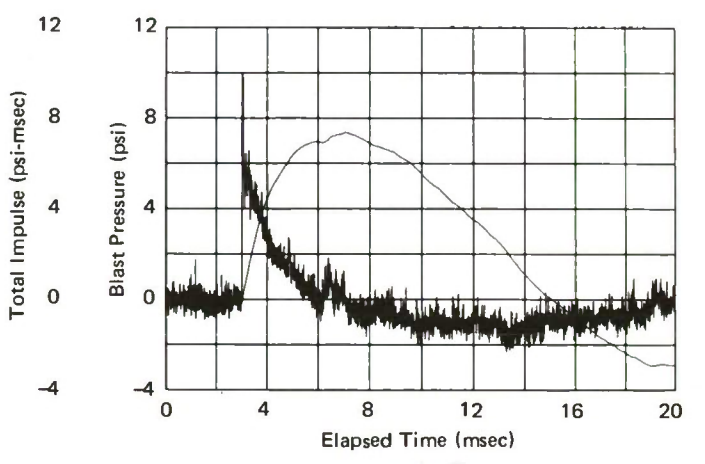

Gage 14

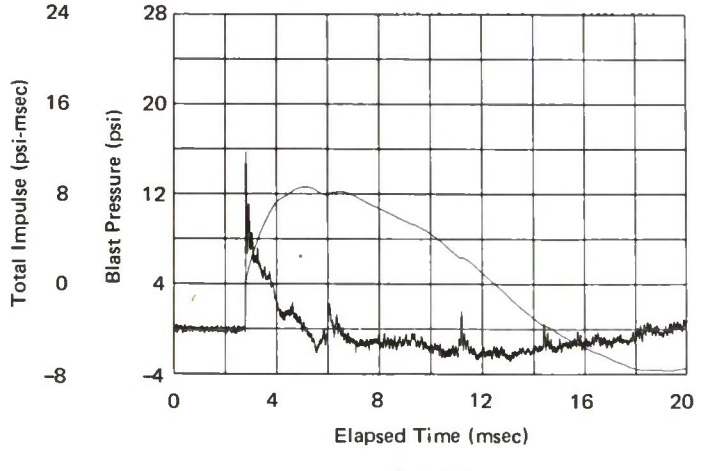

Gage 15

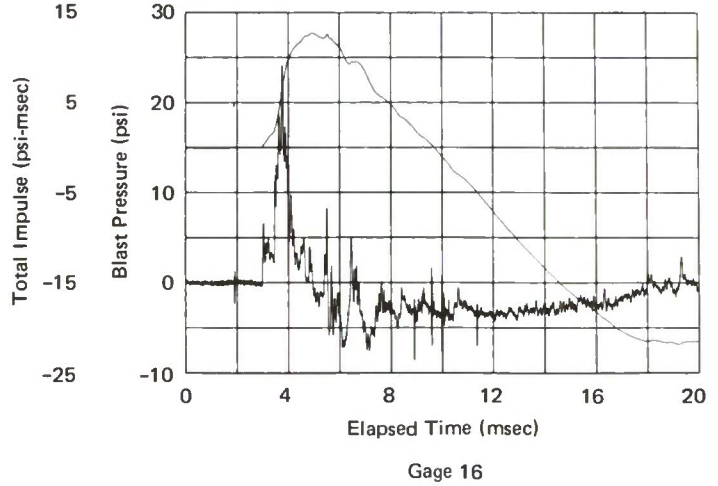

Gage 16

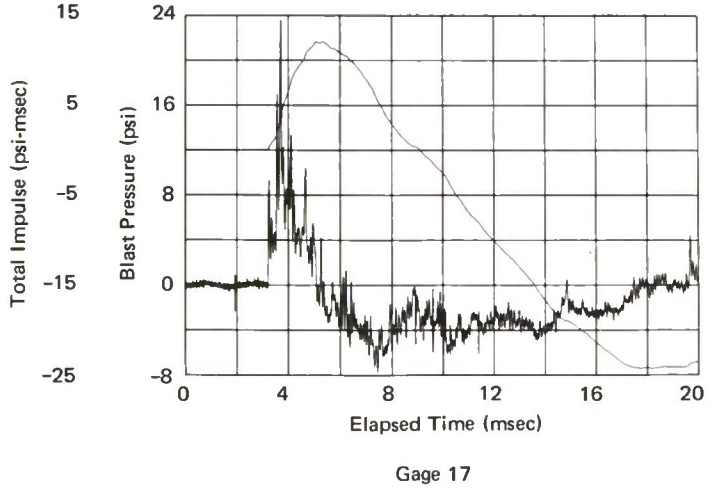

Gage 17

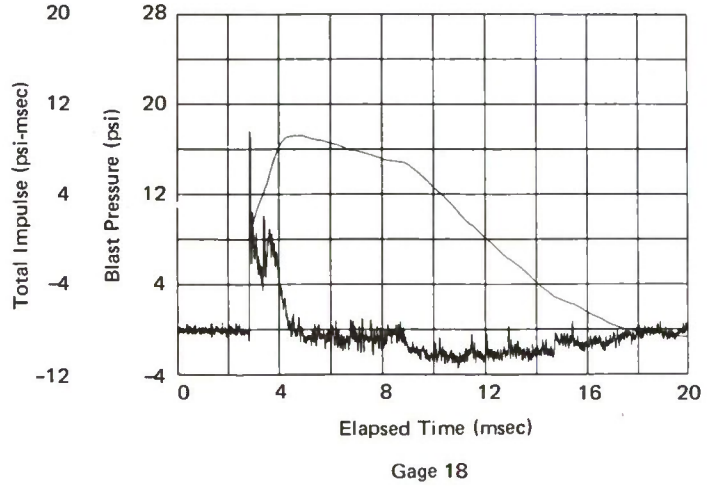

Gage 18

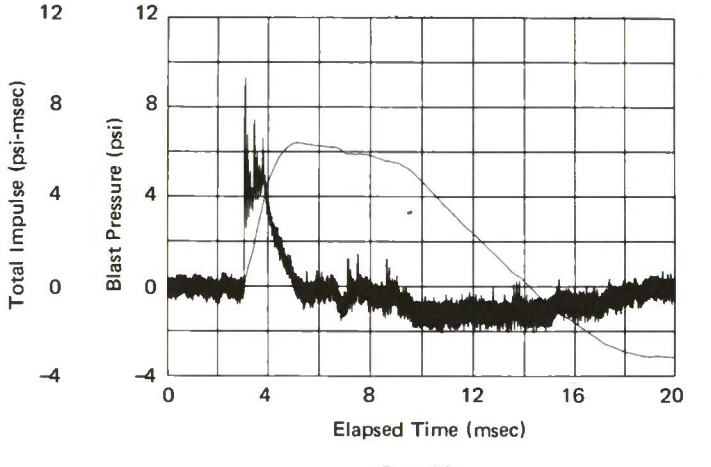

Gage 19

Figure 10. Continued

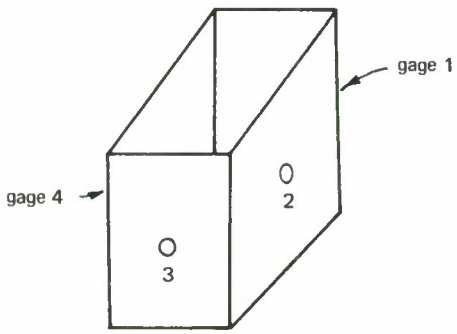

Notes:

1. Angle of incidence = 55 degrees.
2. Gage height = 30 inches.
3. Charge height = 12 inches.
4. Plotted data points represent an average of five values.

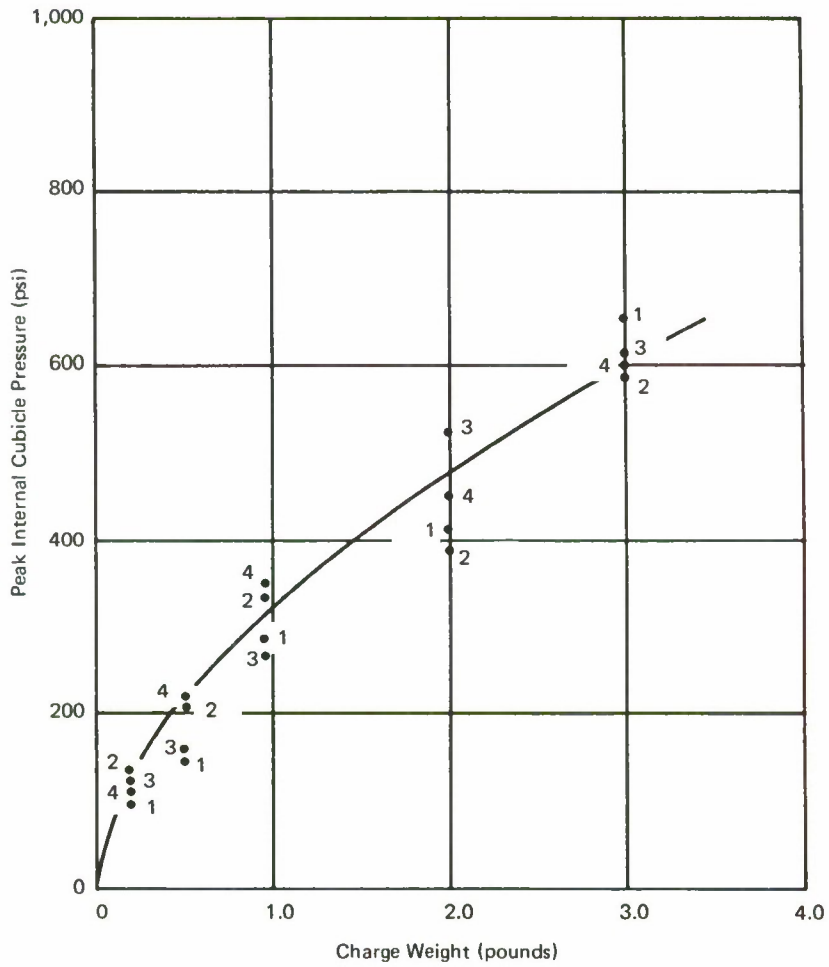

Figure 11. Peak internal cubicle pressure for various charge weights.

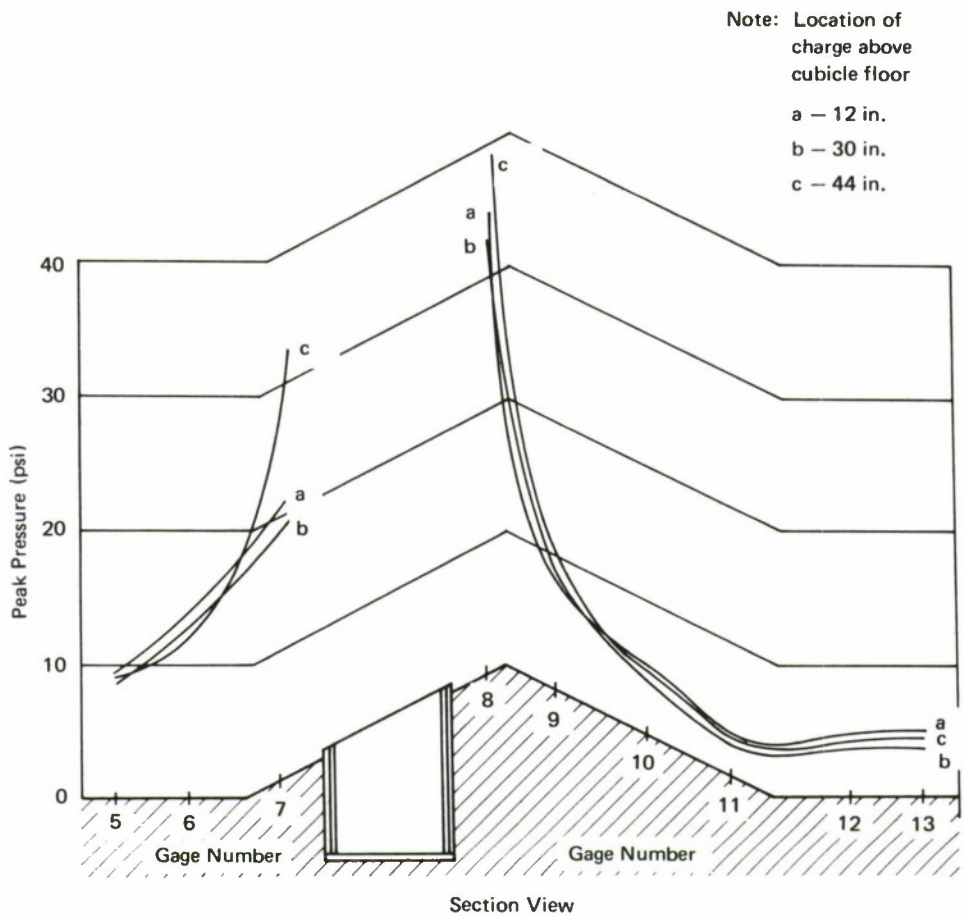

Figure 12. Peak pressures for a 1-pound charge at various heights (gages 5 through 13).

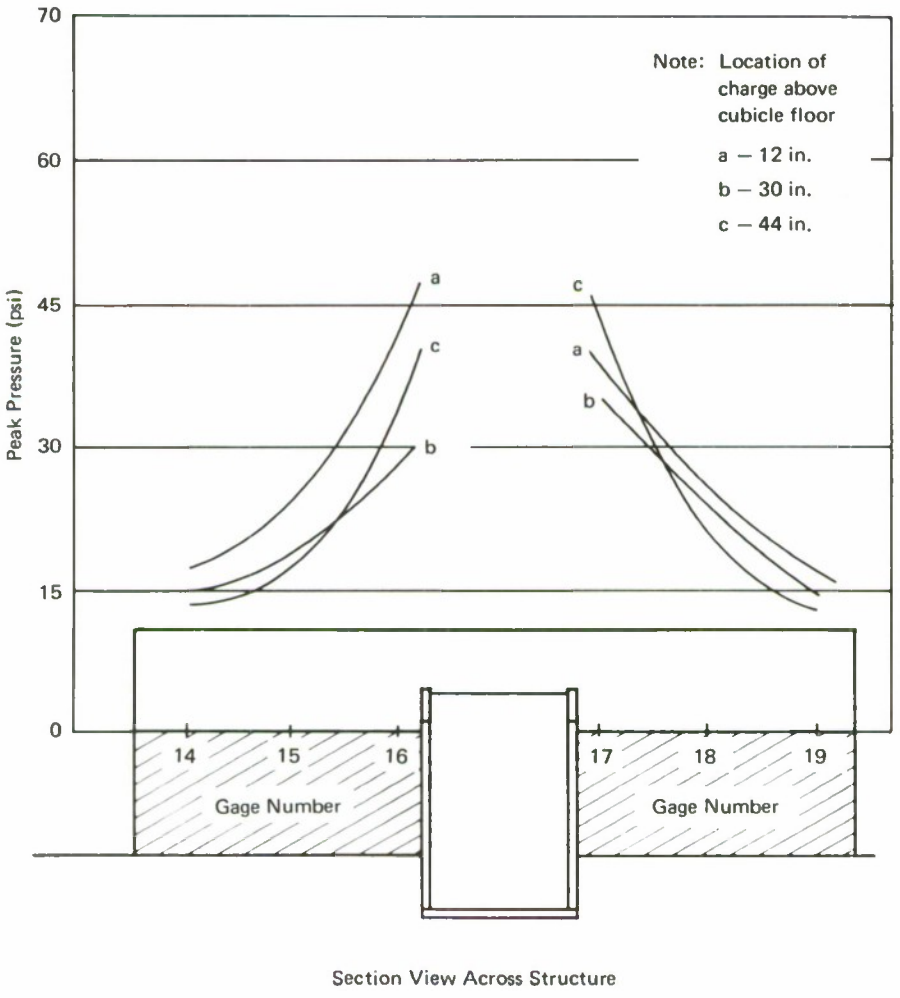

Figure 13. Peak pressures for a 1-pound charge at various heights (gages 14 through 19).

Table 3. Peak Pressures for 1-Pound Charge at Various Charge Heights

Gage	Peak Pressures (psi) for Charge Heights (in.) of—		
	12	30	44
1	242.0	1,264.6	418.2
2	268.2	1,939.9	256.3
3	231.7	1,298.7	196.5
4	273.7	1,676.7	279.3
5	8.83	8.40	8.75
6	14.79	13.96	12.83
7	20.51	19.93	31.20
8	34.40	32.25	38.40
9	7.67	7.80	9.90
10	4.38	3.73	4.30
11	2.79	2.00	2.13
12	4.38	3.74	4.00
13	4.58	3.47	4.20
14	16.90	14.48	13.24
15	23.70	18.39	17.10
16	43.10	26.94	34.16
17	37.20	24.17	43.21
18	25.54	25.26	20.20
19	16.28	14.93	12.70

Table 4. Peak Total Positive Impulses for 1-Pound Charge at Various Charge Heights

Gage	Peak Impulses (psi-msec) for Charge Heights (in.) of—		
	12	30	44
1	192.4	188.0	133.3
2	154.5	200.7	117.1
3	197.8	220.9	127.7
4	217.8	232.6	147.2
5	7.70	8.22	8.10
6	10.66	10.60	11.17
7	7.90	10.85	12.01
8	14.33	13.84	15.36
9	5.73	6.44	7.14
10	3.89	4.42	4.84
11	3.46	3.82	3.89
12	3.10	3.40	3.48
13	2.78	3.06	3.21
14	10.49	12.43	12.93
15	11.68	14.13	14.29
16	14.85	13.43	11.28
17	16.53	9.53	12.60
18	12.56	14.50	16.01
19	10.37	13.05	11.40

Discussion of Test Results

Examination of the pressure histories recorded inside the cubicle indicates that full venting occurred without any gas accumulation; however, multiple shocks were observed as the expanding shock wave reflected off the cubicle walls.* The peak pressures within the cubicle were of the same order of magnitude as would be expected by calculating the side-on overpressure at a gage location multiplied by a reflection factor for the angle of incidence. The magnitudes of the internal pressures recorded on the walls were not affected by the different heights of the walls in that no correlation of peak pressure and gage location was observed in Figure 11. Figure 14 shows the average scaled unit impulse based on data from a previous study;** the scaled impulses obtained from the integration of the pressure records of the gages inside the cubicle are also shown. The difference between the measured values and the curve was not unexpected, because the curve represents an average value for each wall and the data are for specific points—not necessarily at an average point.

The pressures on the structure surrounding the cubicle were not significantly affected by variations in the height of the charge. The pressures on the surrounding structure were observed to increase with increasing charge weight, as would be expected (Figures 8 and 9).

The peak pressures for various charge weights were divided by the peak pressures for the lowest charge weight (0.19 pound—equivalent to two 81-mm mortars) to form pressure ratios, P_1/P_2. These pressure ratios were plotted against charge weight ratios, W_1/W_2 (Figure 15). Figure 15 gives the scaling exponents to relate changes in pressure at a point on the structure with changes in the charge weight. The geometry of the structure results in four scaling regions; each of these regions is characterized by a different pressure–weight relationship. Conventional weight–distance scaling for a constant pressure is not applicable to a fixed-geometry problem. The relationships shown are approximate and give orders of magnitude rather than exact values.

Figures 8 and 9 show that except for the close-in gages the pressures resulting from the simultaneous detonation of three 0.19-pound charges 7 inches apart closely approximates the pressures from a single charge of the same total weight. Once the individual shock waves merge, the resulting shock wave approximates that of a single charge.

---

* The multiple reflections increase the duration of the pressure pulse beyond the normal expected duration and increase the impulse significantly. However, this phenomena is believed to be different than gas accumulation pressure from lack of venting although the effect, an increase in impulse, is the same.

** Naval Facilities Engineering Command. NAVFAC P-397: Structures to resist the effects of accidental explosion. Washington, D. C., June 1969. (Also Army TM-5-1300; AFM-88-22).

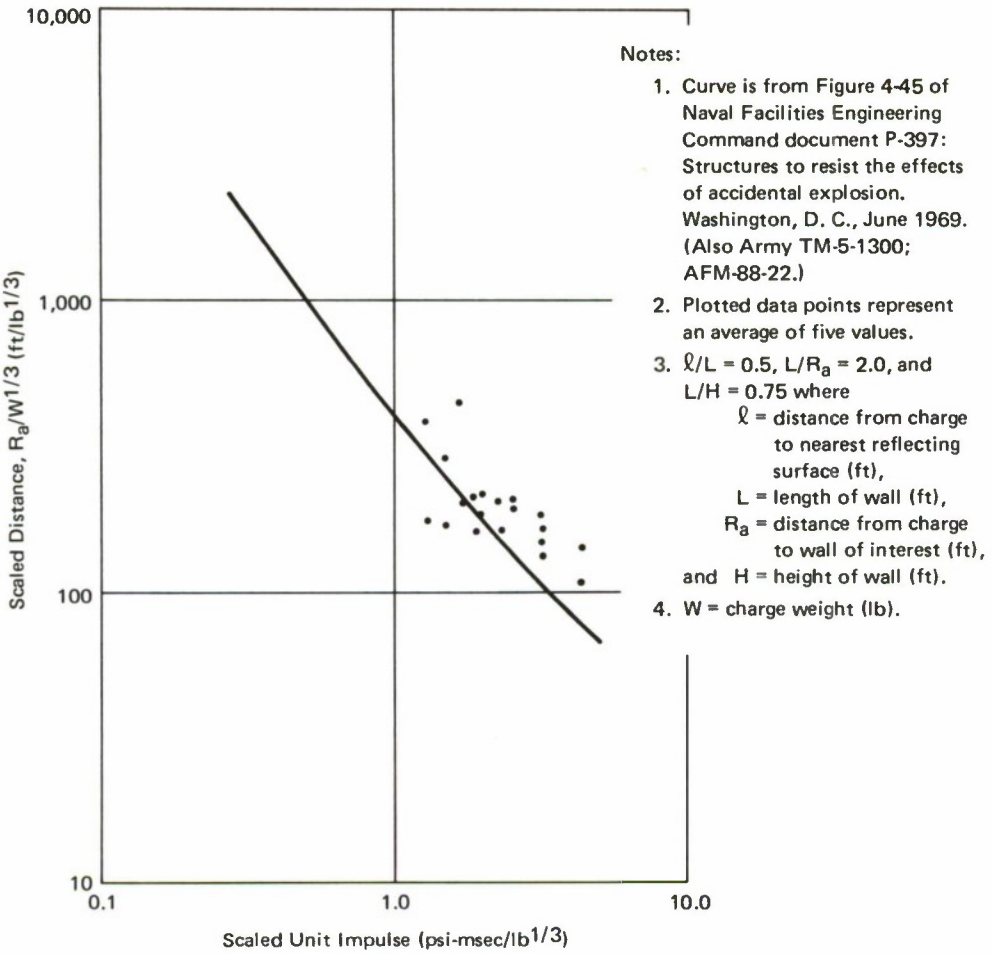

Figure 14. Scaled unit impulse for various scaled distances.

An examination of the pressure histories on the structure surrounding the cubicle (Figure 10) reveals that multiple peaks occurred. These were caused by multiple reflections of the expanding shock wave within the cubicle spilling onto the surrounding structure. Figure 10 shows that as the distance from a point to the charge is decreased, the peak positive pressure, the peak positive impulse, and the peak negative pressure increase (see gages 14 through 19). The long-duration negative phase results in some cases in the total impulse becoming negative; also as the distance between a point and the charge is decreased the total impulse increases in magnitude. The peak negative impulse may be much greater than the peak positive impulse (see gages 16 and 17).

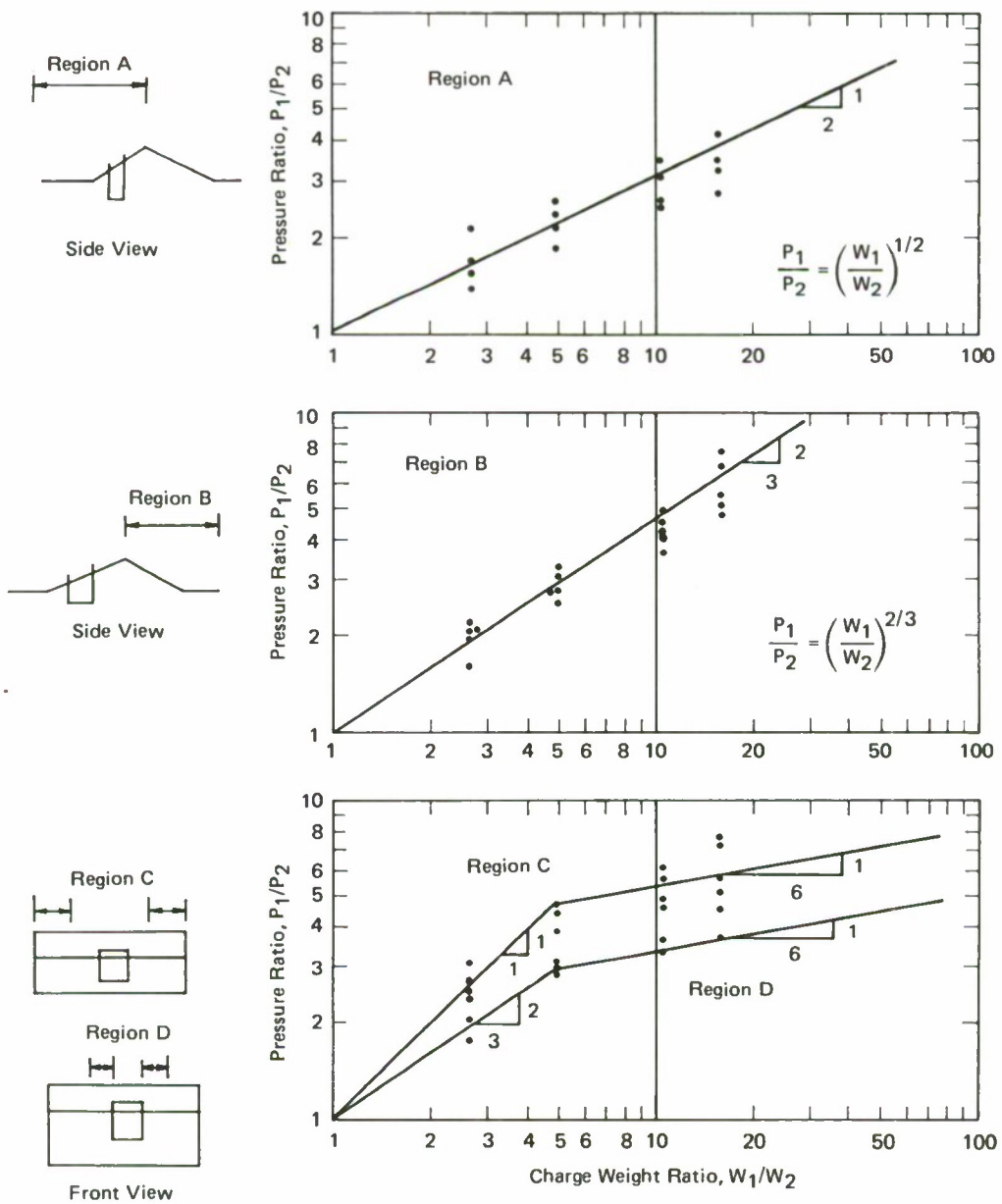

Figure 15. Pressure ratio versus charge weight ratio for regions of structure.

The pressure histories which show relatively long-duration negative pressures of 2 to 3 psi impose a lifting suction on the roofing. The long-duration negative phases result in negative total impulses. This can be understood by considering the formation and passage of a shock wave. An explosion transfers energy into the air, resulting in a compressional air wave. The air wave forms a moving shock front. The pressure behind the shock front is less than that of the front, decaying as a result of spherical expansion, heat transfer, and energy losses. With the passing of the shock front, a wave of rarefaction follows. At a point a specific distance from the explosion, a rise in pressure would be observed, followed by lower pressures. The inertia of the mass of air particles in the shock front overcompresses the air, causing a reversal of direction of the particles. Adjacent air particles also reverse direction, preventing the formation of a partial vacuum. Thus, increasingly negative pressures are superimposed on the trailing end of the positive phase. This negative pressure, when combined with the rarefaction phase, produces a negative phase if the resultant pressure is less than the ambient atmospheric pressure. The area in the negative phase of a pressure–time curve may exceed the area in the initial positive phase, resulting in a negative total impulse at that point. It is also possible for a second positive shock to occur after the negative phase.

BLAST ENVIRONMENT—PARTIALLY VENTED CUBICLE

Approach

The pressures on the structure surrounding the fully vented protective cubicle tested earlier were found to be relatively high compared with allowable limits on conventional structures. Several methods were tried to reduce the pressure acting on the exterior of the surrounding structure. This phase of the work was divided into two parts simulating the effects of:

1. The detonation of six 81-mm projectiles within a cubicle containing a roof with a reduced venting area.
2. The detonation of six 81-mm projectiles within a cubicle containing a roof with a venting pipe.

The tests were conducted on the same one-third scale model used earlier; the same instrumentation was used.

Test Procedure

Structure. The protective cell used earlier was modified by welding a 3-inch steel plate acting as a roof. The plate contained a 2-foot-diameter hole for venting of the blast. Additional plates were bolted to the roof to reduce the venting area. A 6-inch-outside-diameter pipe (internal diameter of 4.9 inches) was later attached to the roof to further reduce and direct venting of the blast.

Explosive Charges. Throughout this phase the six 81-mm projectiles were represented by a 0.50-pound cylinder of composition B.

Results of Blast Tests

The following tests were conducted:

Number of Shots	Charge Size (lb)	Description
5	0.50	2-foot-diameter venting area in roof
5	0.50	7-inch-diameter venting area in roof
5	0.50	4.5-foot by 6-inch-diameter* pipe attached to roof
5	1.00	4.5-foot by 6-inch-diameter* pipe attached to roof
5	0.50	9-foot by 6-inch-diameter* pipe attached to roof

* 4.9-inch inside diameter.

Figures 16 through 18 show the test structure. The charges were located as previously. The peak pressures are given in Table 5 and Figures 19 and 20. Peak impulses are summarized in Table 6. Figure 21 gives typical gas accumulation pressures inside the cubicle for various amounts of venting.

Discussion of Test Results

Figure 22 shows the pressure histories for different amounts of venting; note the increased duration of the pressure as the venting area is reduced. The duration of the gas pressure is primarily a function of the vent area–cubicle volume ratio; Figure 23 shows the relationship for the cubicle under study. The magnitude of the gas build-up is primarily a function of the charge weight–cubicle volume ratio. Figure 21 shows the gas pressure observed in the test is very close to that predicted from the curve.

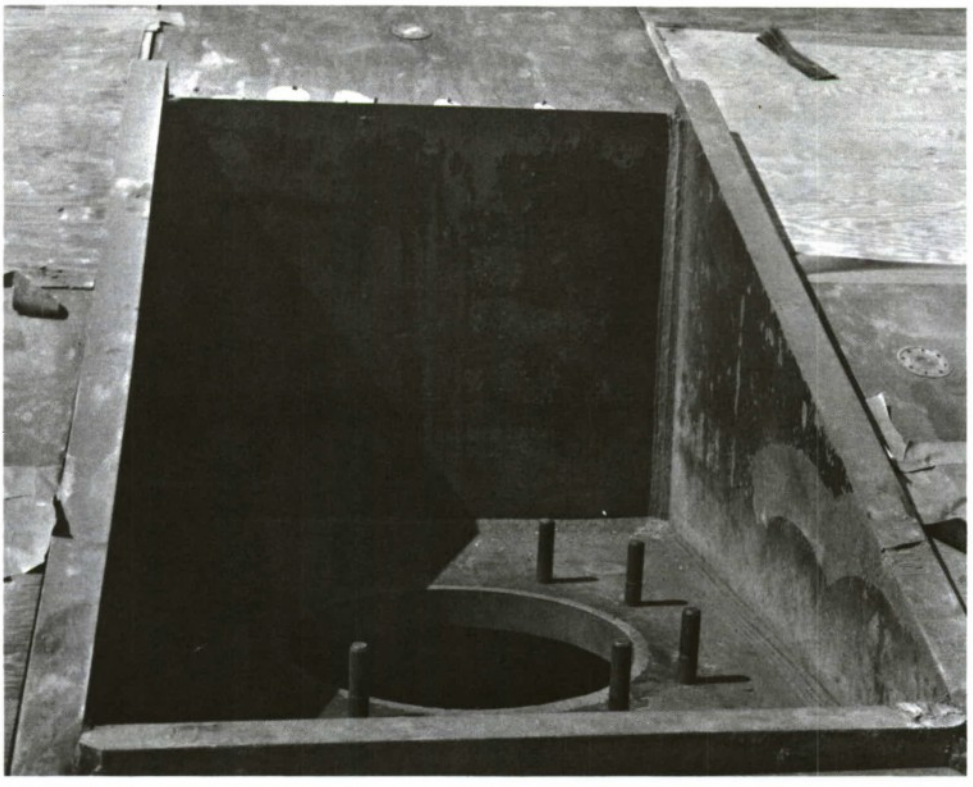

Figure 16. Cubicle roof with 2-foot-diameter venting hole.

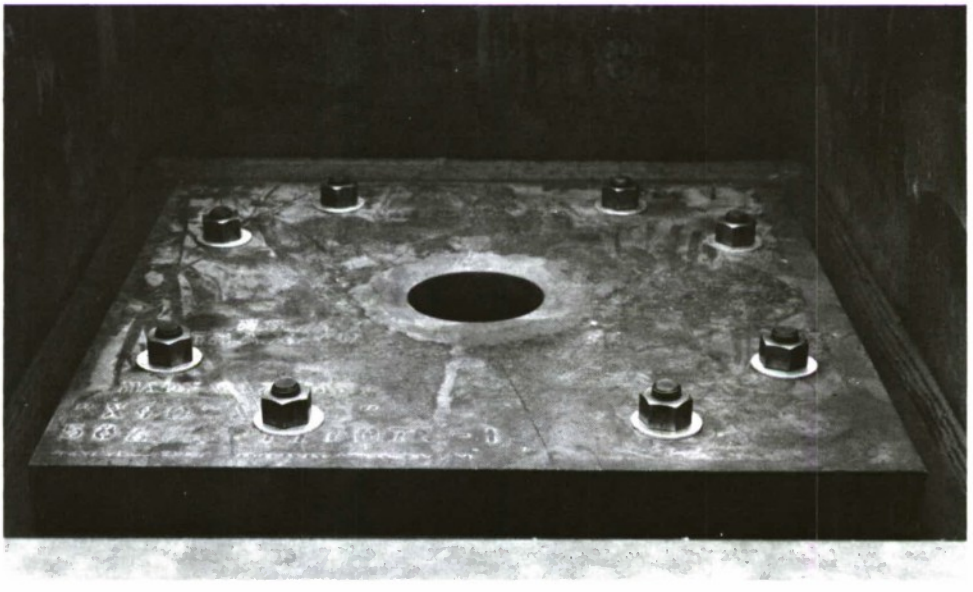

Figure 17. Roof cover plate with 7-inch-diameter venting hole.

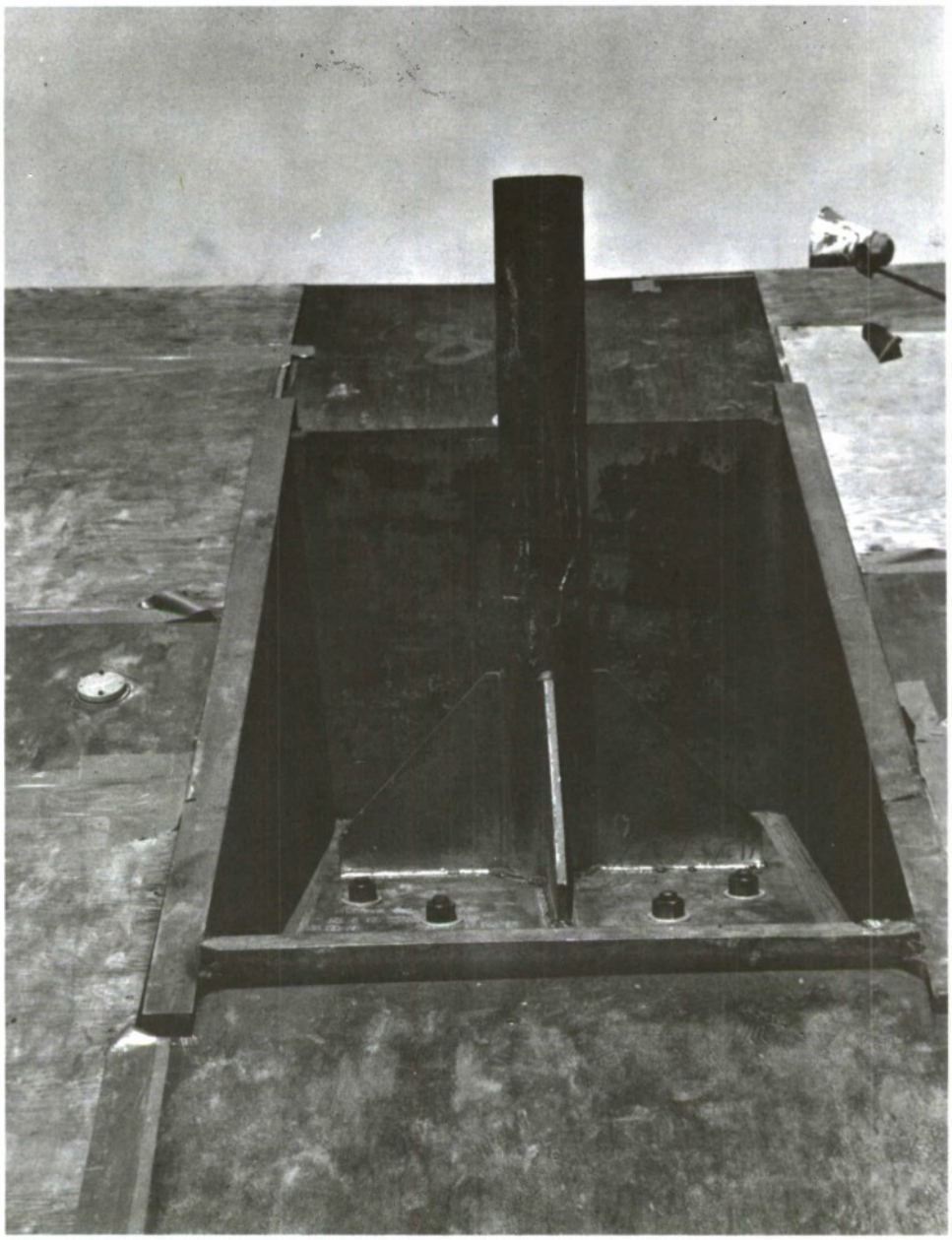

Figure 18. Venting stack, 4.5 feet by 4.9 inches in inside diameter.

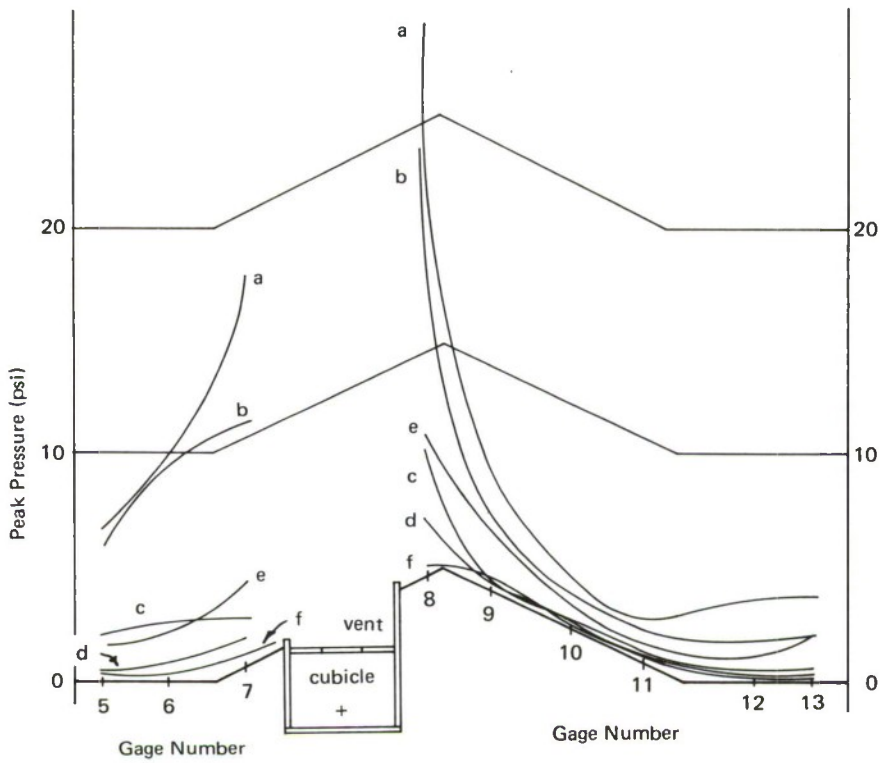

a — Full venting
b — 2-ft diam vent
c — 7-in. diam vent
d — 4.9-in. diam stack 4.5-ft long
e — 4.9-in. diam stack 4.5-ft long, 1.0 lb charge
f — 4.9-in. diam stack 9-ft long

Note: All charge weights 0.50 lb except where noted.

Figure 19. Peak pressures for various venting configurations (gages 5 through 13).

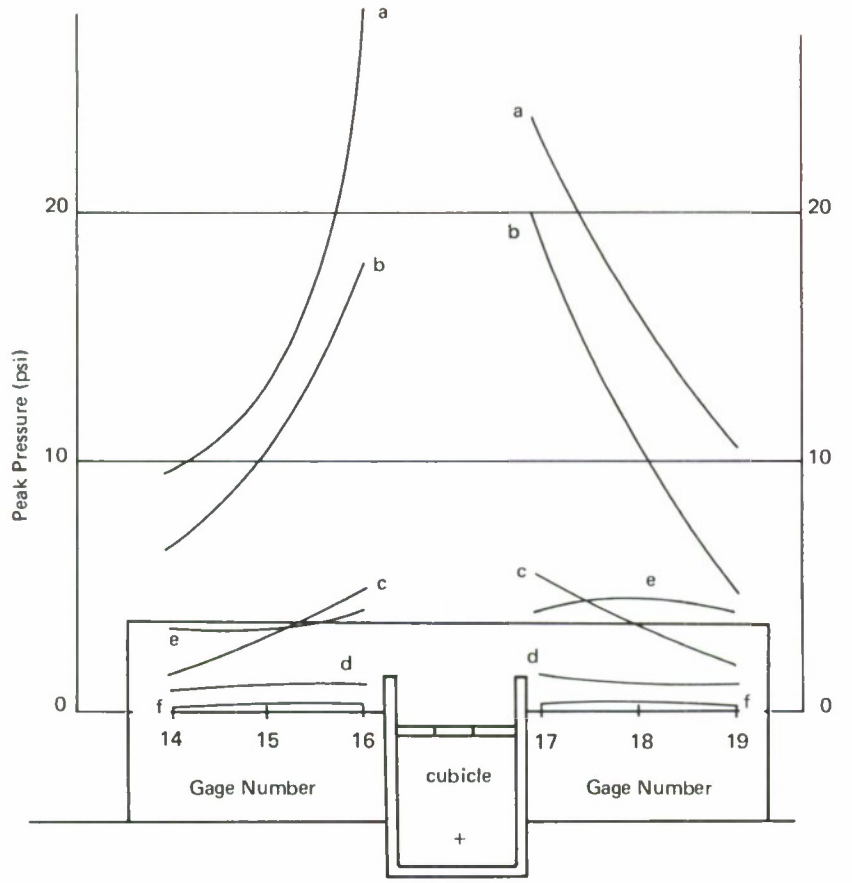

a — Full venting
b — 2-ft diam vent
c — 7-in. diam vent
d — 4.9-in. diam stack 4.5-ft long
e — 4.9-in. diam stack 4.5-ft long, 1.0 lb charge
f — 4.9-in. diam stack 9-ft long

Note: All charge weights 0.50 lb except where noted.

Figure 20. Peak pressures for various venting configurations (gages 14 through 19).

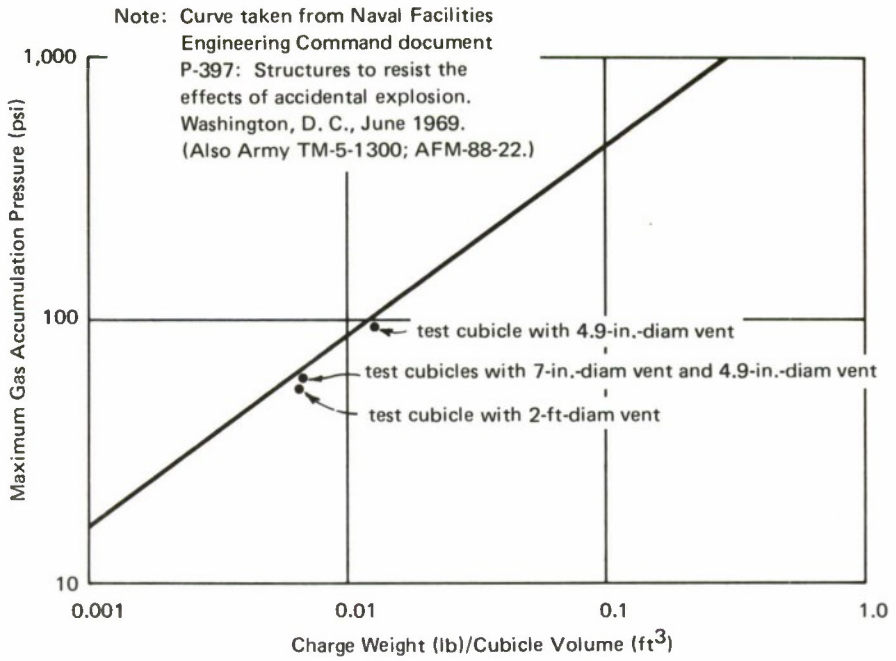

Figure 21. Gas pressure versus weight—volume ratio.

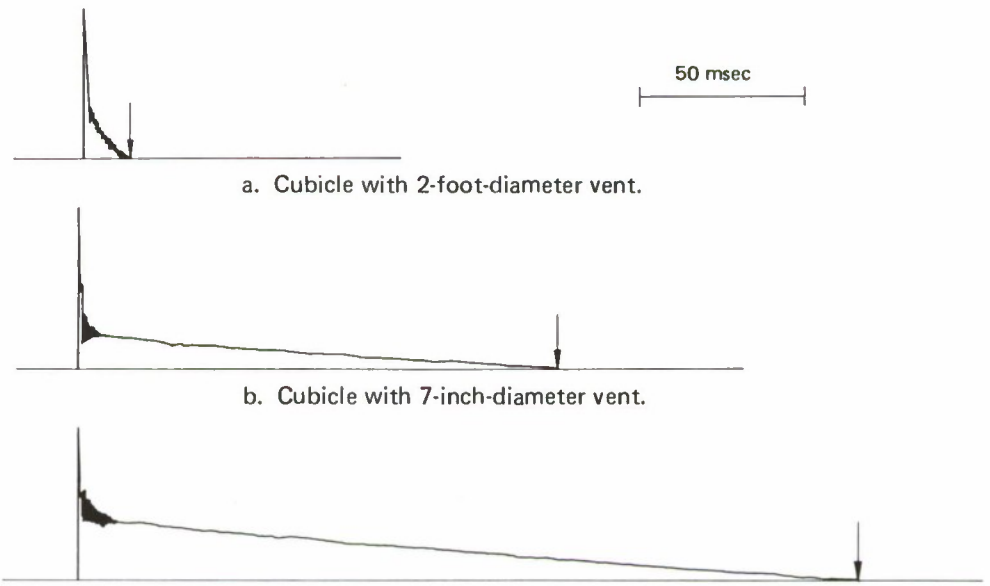

a. Cubicle with 2-foot-diameter vent.

b. Cubicle with 7-inch-diameter vent.

c. Cubicle with 4.9-inch-diameter vent pipe

Figure 22. Pressure—time curves for various venting configurations.

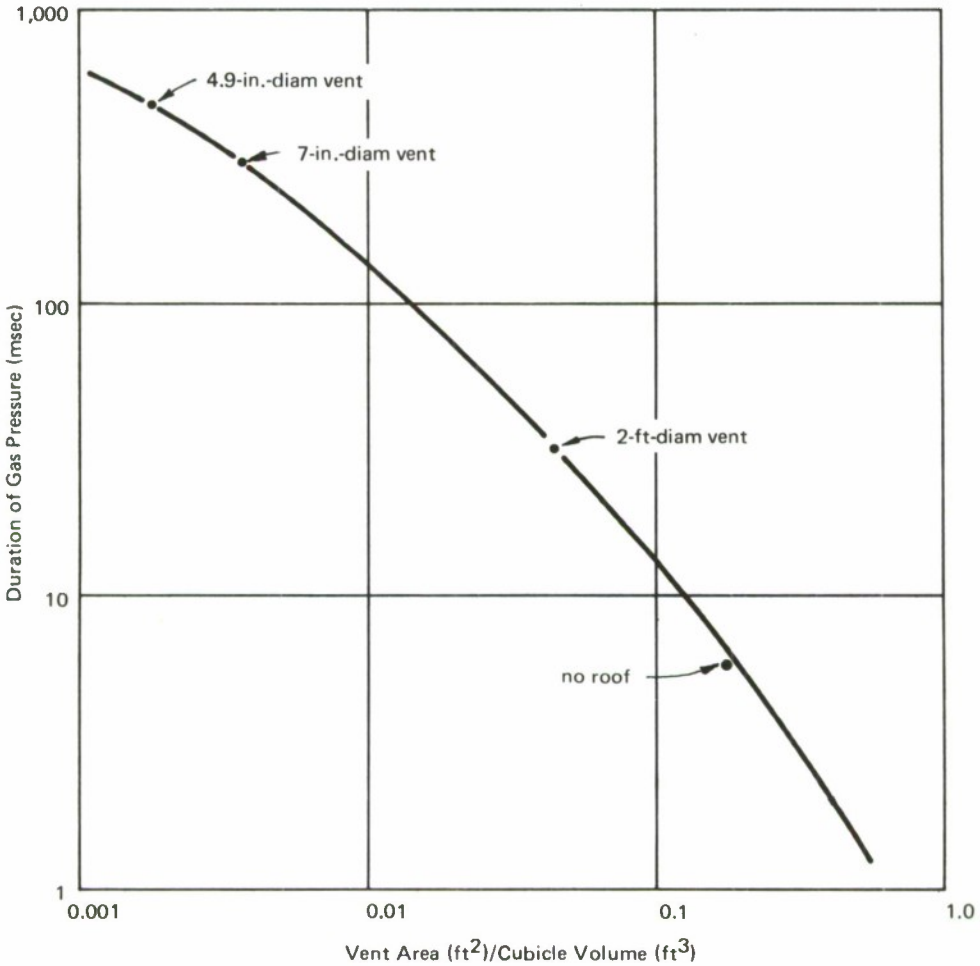

Figure 23. Blast duration time versus area–volume ratio.

Table 5. Summary of Average Peak Pressures

Gage	Average Peak Pressures (psi) for Conditions of—				
	2-Foot-Diam Venting; 0.5-Pound Charge	7-Inch-Diam Venting; 0.5-Pound Charge	4.5-Foot-Long by 4.9-Inch-Diam[a] Venting; 0.5-Pound Charge	4.5-Foot-Long by 4.9-Inch-Diam[a] Venting; 1.0-Pound Charge	9-Foot-Long by 4.9-Inch-Diam[a] Venting; 0.5-Pound Charge
1	157.2	180.5	159.2	303.6	222
2	235.0	252.3	205.6	430.4	252
3	170.3	161.7	171.1	335.2	199
4	207.3	209.1	217.1	427.7	169
5	6.08	1.61	0.43	0.68	0.31
6	9.48	2.28	0.61	1.03	0.24
7	10.49	1.84	1.13	1.09	0.24
8	18.11	5.08	2.38	3.82	0.65
9	3.04	0.37	0.23	0.49	0.85
10	1.57	0.22	0.14	0.32	[b]
11	1.43	0.22	0.15	0.27	0.36
12	1.57	0.22	0.15	0.35	[b]
13	1.46	0.29	0.20	0.32	0.33
14	5.06	1.52	0.79	1.23	0.21
15	5.18	2.81	1.06	1.83	0.27
16	16.54	4.00	1.21	1.79	0.32
17	18.35	5.30	1.46	1.99	0.32
18	10.88	3.07	0.98	2.11	[b]
19	4.84	1.89	0.94	1.47	[b]

[a] Inside diameter of pipe. Outside diameter was 6 inches.

[b] Data not recorded during test.

Table 6. Summary of Average Peak Impulses

Gage	Average Peak Total Positive Impulse (psi-msec) for Conditions of—				
	2-Foot-Diam Venting; 0.5-Pound Charge	7-Inch-Diam Venting; 0.5-Pound Charge	4.5-Foot-Long by 4.9-Inch-Diam[a] Venting; 0.5-Pound Charge	4.5-Foot-Long by 4.9-Inch-Diam[a] Venting; 1.0-Pound Charge	9-Foot-Long by 4.9-Inch-Diam[a] Venting; 0.5-Pound Charge
1	523.2	5,784	9,300	14,850	10,604
2	450.7	5,979	10,329	16,030	13,258
3	444.7	6,488	11,739	19,870	9,485
4	474.3	5,683	9,432	15,400	10,793
5	3.15	0.44	0.10	0.21	0.044
6	3.87	0.43	0.16	0.25	0.046
7	4.96	0.66	0.30	0.55	0.050
8	7.60	1.48	0.42	0.78	0.063
9	2.14	0.36	0.12	0.20	0.082
10	1.69	0.29	0.10	0.21	[b]
11	1.51	0.25	0.08	0.20	0.012
12	1.42	0.23	0.07	0.18	[b]
13	1.15	0.21	0.10	0.09	0.030
14	3.78	0.54	0.15	0.30	0.063
15	5.03	0.71	0.20	0.36	0.056
16	10.50	1.53	0.17	0.34	0.050
17	10.30	1.56	0.18	0.52	0.030
18	5.61	0.85	0.21	0.57	[b]
19	3.18	0.57	0.18	0.29	[b]

[a] Inside diameter of pipe. Outside diameter was 6 inches.
[b] Data not recorded during test.

The pressures on the surrounding structure were characterized by multiple reflections with maximum pressures not necessarily occurring on the first peak. This fact explains the increased spread of peak values when compared with previous data.

The pressures on the surrounding structures were reduced to a marginally safe level for conventional construction by use of the 7-inch-diameter venting hole in the roof. The 9-foot-long by 6-inch-diameter venting pipe reduced the pressures on the surrounding structure to a safe level. The increased gas accumulation within the cubicle significantly increases the duration of the loading and the impulse acting on the cubicle walls. This changes the nature of the loading within the cubicle to that of a long-duration load rather than of a pure impulse.

FRAGMENT VELOCITY DETERMINATION

Approach

One of the objectives of the test program was the determination of the velocity of secondary fragments produced by the breakup of processing equipment used in the protective cells. Typical equipment items found in a protective cell include drill machines, conveyor systems, pallets, etc. This portion of the test program was conducted in full scale with actual 81-mm mortar rounds. The approach taken was to place selected pieces of machinery, representative of the processing machines and conveyor elements found in the protective cell, around 81-mm projectiles and to detonate the projectiles. The velocities of the secondary fragments were determined by high-speed camera coverage and backboards consisting of layers of insulating board.

Test Procedure

Three shots were conducted with the same test setup. The first two shots had two 81-mm projectiles; the third shot had ten 81-mm projectiles. The projectiles were placed on a conveyor table, 20 inches above ground, and selected pieces of machinery were placed around them. Three high-speed cameras were used to record the path of fragments. Two cameras operated at 500 frames per second, and the third operated at 1,000 frames per second. IRIG timing was provided to each camera to determine the actual film speed. The cameras and the detonation circuit were controlled by a program sequencer located in the bunker. The projectiles, type 81-mm HE M374, were defuzed and one ounce of C-4 plastic explosive was placed in the fuze

well; an engineer's special blasting cap was placed in the C-4. The blasting caps were detonated by a high-voltage capacitor discharge circuit connected through the program sequencer. Power was provided to the cameras and firing circuit from portable electric generators. Four backboards, 8 feet high by 4 feet wide, each consisting of 32 layers of 1/2-inch cellulose-fiber wallboard, were placed next to each other to form a wall 25 feet away from the projectiles. Figures 24 through 28 show the test setup.

Postshot Fragment Distribution

Postshot distribution of machine parts and fragments which were observed and could be identified are shown in Tables 7a through 7d. Most of the machine parts were shattered or fractured, making recovery very difficult. An area 600 feet by 400 feet was searched in an attempt to find fragments. Despite reasonable care, several items were not found.

Several preshot and postshot photographs show the severity of the breakup of the parts (Figures 29 through 32). Several of the items found at large distances from the charge include: a piece of aluminum manifold (A34) at 250 feet, a steel gear (C20) at 219 feet, and a piece of chain (C27) at 302 feet.

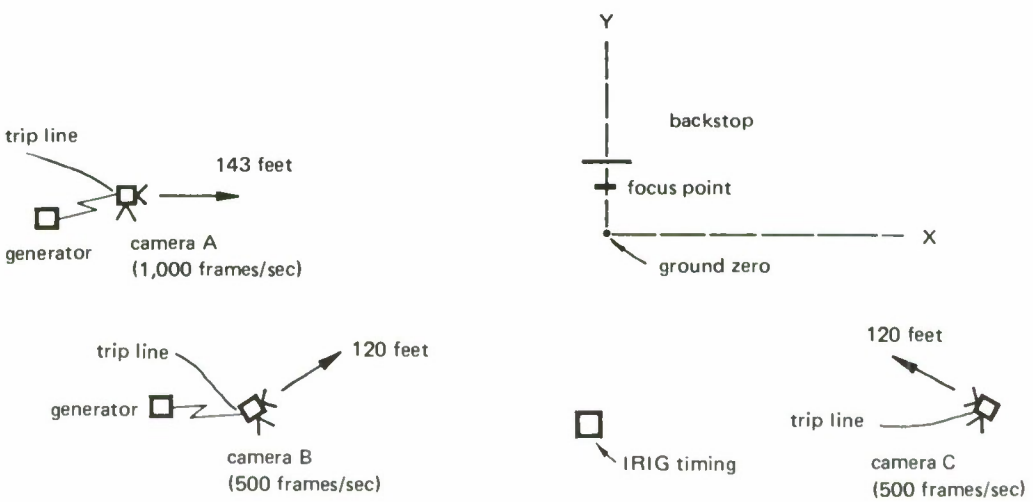

Shot 1: two rounds 11-1/4 inches part.
Shot 2: two rounds 33-3/4 inches apart.
Shot 3: ten rounds each 11-1/4 inches apart.

Figure 24. Test site plan.

Figure 25. High-speed camera position.

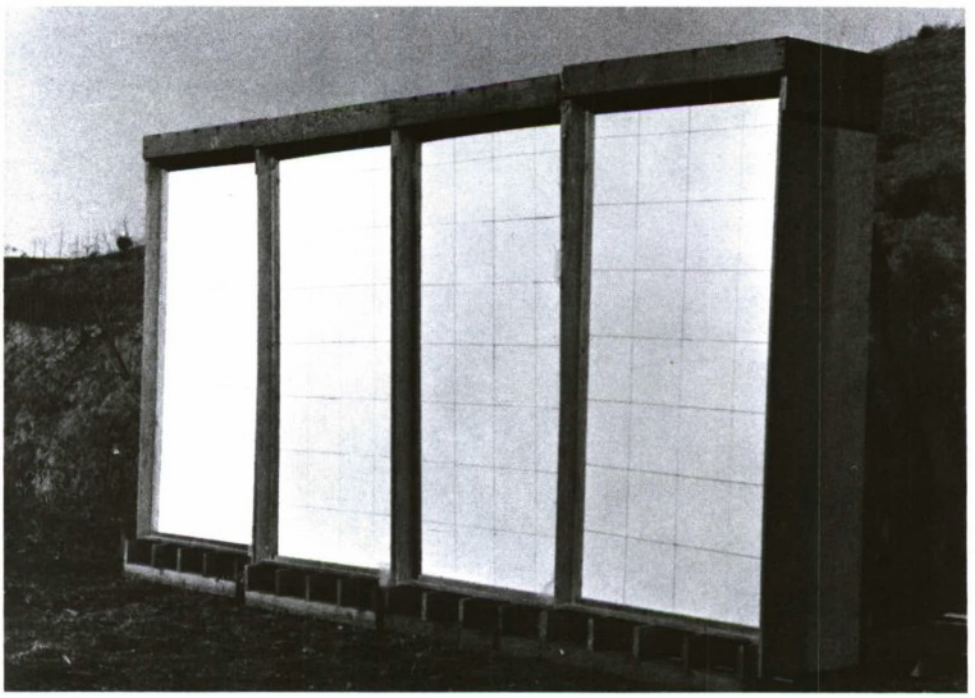

Figure 26. Cellulose-fiber wallboard backstop.

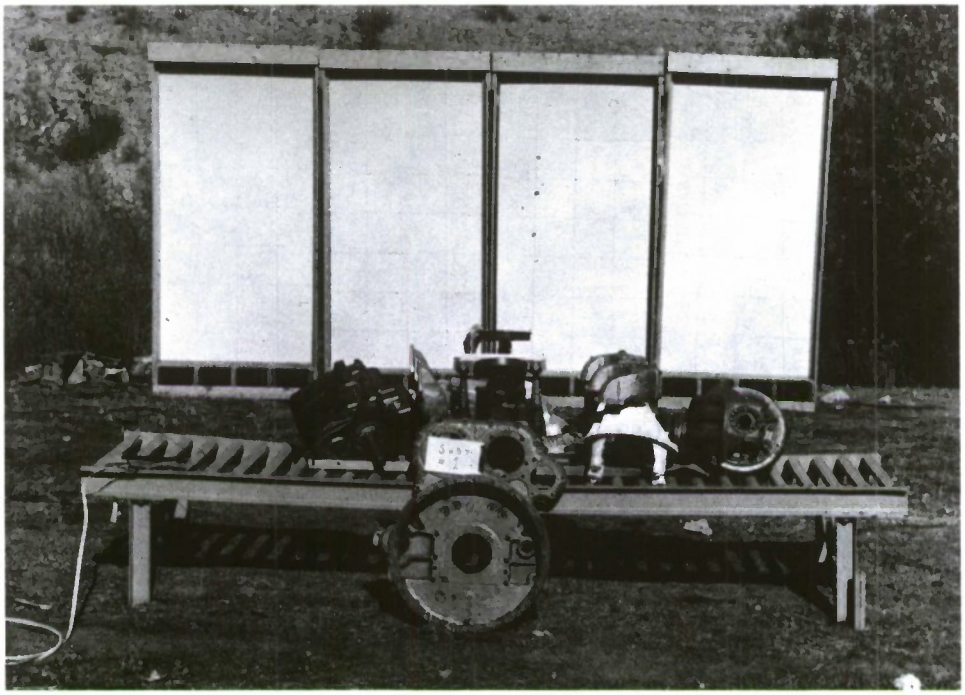

Figure 27. Test setup for shot 1.

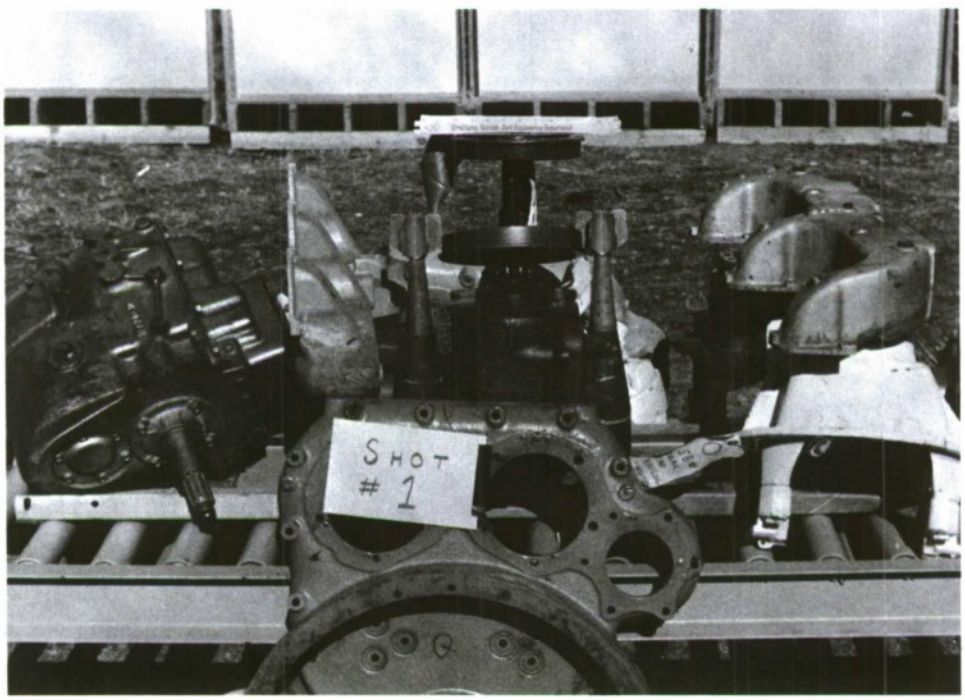

Figure 28. Closeup of test setup for shot 1.

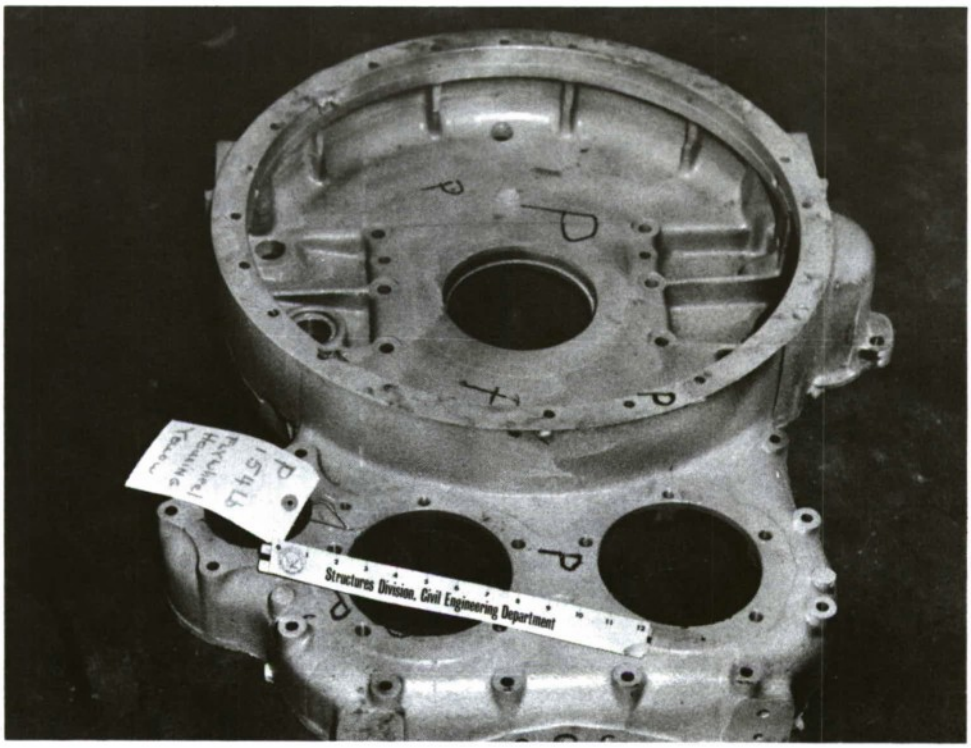

Figure 29. Preshot view of flywheel housing, part P.

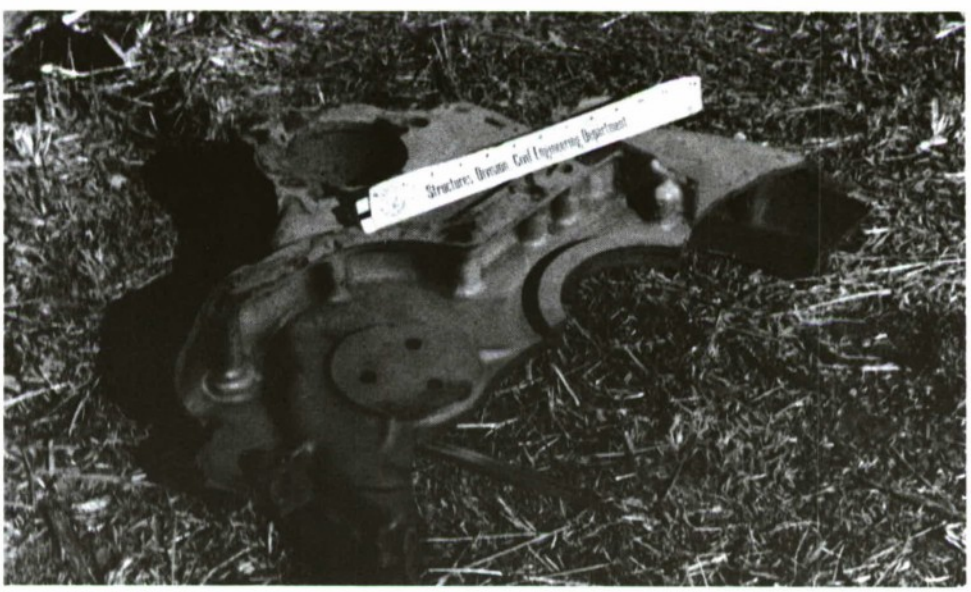

Figure 30. Postshot view of flywheel housing, part P.

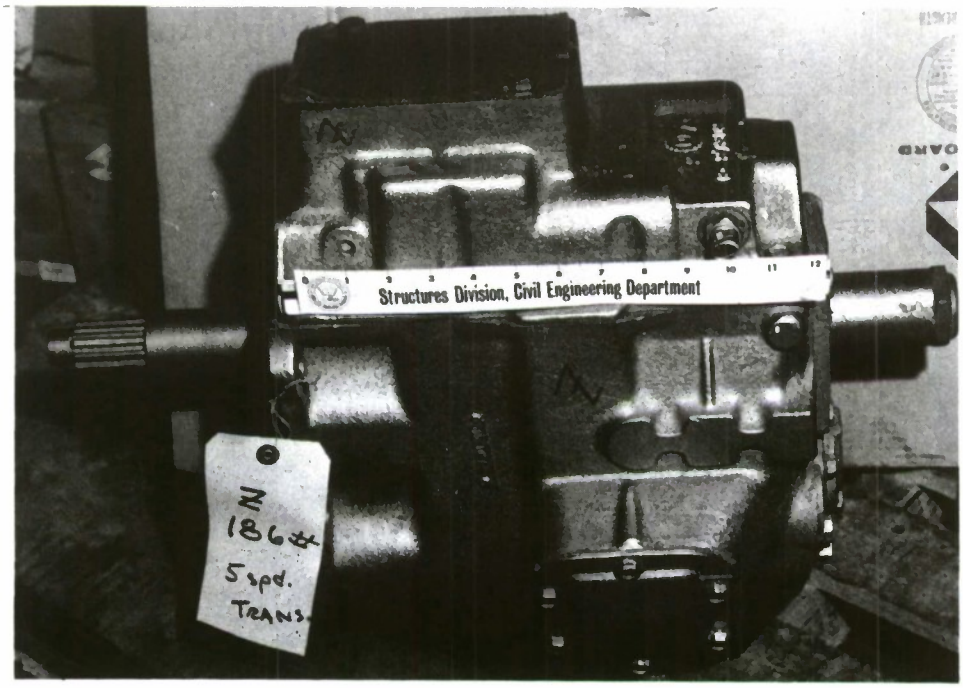

Figure 31. Preshot view of transmission, part Z.

Figure 32. Postshot view of transmission, part Z.

Table 7a. Original Machine Parts

Designation	Description	Color	Weight (lb)
A	pivot block	blue	36
B	steel gear	light gray	36
C	stainless-steel double gear	black	7
D	stainless-steel pressure regulator	olive drab	18
E1	cast wheel with shaft	red	15
E2	cast wheel with shaft	red	12
E3	cast wheel with shaft	red	12
E4	cast wheel with shaft	red	12
F	steel gear	orange	32
G	ram	silver	7
H1	small clutch plate	gold	5
H2	large clutch plate	gold	15
H3	large clutch plate	gold	13
I	electrical gears	dark gray	8
J1	small universal	white	9
J2	medium universal	white	15
J3	large universal	white	38
K1	aluminum manifold	–	14
K2	aluminum manifold	–	15
L	steel wide-track wheel	green	44
M	small transmission	olive drab	56
N	rear-end housing	red	67
O	small rear-end housing	white	58
P	flywheel housing	yellow	154
Q	flywheel housing	orange	154
R	pinon gear	–	19
S	ring gear	–	23
T1	short shaft	–	16
T2	short shaft	–	16
T3	short shaft	–	16
T4	short shaft	–	16
U1	chain	–	5.5
U2	chain	–	5.5
U3	chain	–	5.5
U4	chain	–	5.5
U5	chain	–	5.5
V	motor coil	yellow	10
W	8-inch angle plate	red	3.5
X	2-inch-diameter by 6-inch pipe	red	1.5
Y	piston rod	black	7
Z	five-speed transmission	gold	186
AA	rear end	blue	203
BB	five-ton hoist	–	360
CC	shock absorber	green	11
DD1	sheet metal	–	12
DD2	sheet metal	–	12

Table 7b. Postshot Location of Pieces After Shot 1

Piece Designation	Description	Weight (lb)	X Distance (ft)	Y Distance (ft)
A4	roller from conveyor	6.0	-2	11
A5	chain	2.70	-10	7
A6	flywheel housing	7.33	1	14
A7	piece flywheel housing, part P	70[a]	5	23
A8	piece flywheel housing, part P		-3	22
A9	short shaft, part T1	16.0	-3	[b]
A10	piece flywheel, part P	4.61	4	24
A11	piece flywheel, part P	0.90	4	25
A12	medium universal, part J2	15.0	14	4
A13	rear end, part AA	203	13	-5
A14	piece flywheel, part P	6.60	46	-80
A15	rear end, part O	58	35	-35
A16	end of piston rod, part Y	0.82	35	-75
A17	gear	5.99	0	-68
A18	gear	0.63	0	-67
A19	gear	1.32	-3	-65
A20	wheel, part E4	12	-3	-69
A21	gear	0.70	-11	-75
A22	piece flywheel, part O	2.71	12	-36
A23	piece flywheel, part Q	100[a]	-2	-19
A24	piece transmission, part Z	3.16	-4	-29
A25	piece transmission, part Z	3.06	-20	-3
A26	piece transmission, part Z	8.72	-24	0
A27	piece transmission, part Z	120	-36	-2
A28	piece transmission, part Z	1.42	-28	-3
A29	piece transmission, part Z	4.35	-32	-8
A30	piece transmission, part Z	1.42	-79	-38
A31	piece transmission, part Z		-79	-60
A32	piece aluminum manifold, part K	0.35	-101	-40
A33	piece aluminum manifold, part K	0.72	-179	-15
A34	piece aluminum manifold, part K	0.14	150	200
A35	piece aluminum manifold, part K	0.31	90	200

[a] Estimated weight.

[b] Struck backstop.

Table 7c. Postshot Location of Pieces After Shot 2

Piece Designation	Description	Weight (lb)	X Distance (ft)	Y Distance (ft)
B1	piece flywheel, part P	70	5	23
B2	rear-end housing, part O	58	5	24
B3	medium universal, part J2	15	5	[b]
B4	cast wheel, part E2	12	-2	24
B5	piece of sprocket	0.67	-1	22
B6	piece flywheel, part P	2.20	-3	25
B7	conveyor table roller	2.34	-4	25
B8	piece flywheel, part P	6.20	-8	25
B9	shaft from transmission	6.77	-10	[b]
B10	piece flywheel, part P	5.43	-15	8
B11	piece transmission	1.50	-29	14
B12	piece transmission	25[a]	-10	0
B13	rear end, part AA	200[a]	21	1
B14	flywheel housing, part Q	100[a]	36	-2
B15	conveyor table roller	5.67	27	14
B16	conveyor table roller	6.0	34	19
B17	conveyor table roller	6.0	36	19
B18	piece flywheel, part Q		20	-8
B19	conveyor table roller	6.0	3	-13
B20	conveyor table roller	6.0	-7	-16
B21	piece transmission, part Z	4.25	-26	-20
B22	piece flywheel, part Q	19.5	-54	-45
B23	piece flywheel, part Q	1.5	-130	-75
B24	piece flywheel, part Q		-110	-65
B25	piece chain	1.37	-74	20
B26	piece transmission, part Z	5.04	-49	24
B27	piece transmission, part Z	1.48	-33	3
B28	piece flywheel, part Q	1.33	-75	-36

[a] Estimated weight.
[b] Struck backstop.

Table 7d. Postshot Location of Pieces After Shot 3

Piece Designation	Description	Weight (lb)	X Distance (ft)	Y Distance (ft)
C1	conveyor table roller	6.41	-6	[b]
C2	steel gear, part F	24	-5	[b]
C3	chain		-5	[b]
C4	chain	0.63	-2	[b]
C5	piece gear, transmission, part Z	34.5	-1	[b]
C6	cast wheel, part E3	12	-3	[b]
C7	piece conveyor table	0.37	-1	[b]
C8	chain	0.76	2	[b]
C9	steel wheel, part L	44.0	7	[b]
C10	piece rear-end housing, part O	42.0	5	[b]
C11	conveyor table roller	6.59	4	[b]
C12	ring gear, part 5	22	1	[b]
C13	piece hoist, part BB	250[a]	0	17
C14	pinion, part R	19	2	9
C15	clutch plate, part H1	5	3	10
C16	clutch plate, part H2	15	-1	7
C17	piece conveyor table	50[a]	0	6
C18	shock absorber, part CC	11	14	7
C19	piece conveyor table	50[a]	-3	-5
C20	steel gear, part B	34.5	218	6
C21	cast wheel, part E2	12	24	-60
C22	conveyor table roller	6	11	-41
C23	rubber matting		55	9
C24	piece flywheel, part Q	8.96	-6	34
C25	piece flywheel, part Q	5.39	18	-55
C26	piece aluminum sheet	0.96	-81	25
C27	piece chain	1.12	-300	-32
C28	metal piece	0.97	-165	10
C29	large universal, part J3		25	35
C30	cast wheel, part E1	15	60	225
C31	cast wheel, part E3	12	10	200
C32	conveyor table roller	6	10	200
C33	piece manifold		-150	200

[a] Estimated weight.

[b] Struck backstop.

Results of Backstop Penetrations

The Ballistic Analysis Laboratory* has conducted tests to calibrate the penetration of fragments into a specific brand of wallboard to determine fragment velocity. An empirical fit to the data for steel fragments resulted in the following equation (from the Ballistic Analysis Laboratory report):*

$$V = 112{,}881\, e^{0.8091}\, M^{-0.938}\, A^{0.9078}\, (\sec \theta)^{0.5419}$$

where V = fragment velocity (fps)

e = penetration into wallboard (in.)

M = mass (grains)

θ = angle between trajectory and normal to wallboard surface (deg)

A = average presented area (sq in.)

This equation was used to analyze the penetrations in the backstops.

The wallboard used in this test was NU-WOOD STA-LITE white interior finish cellulose-fiber insulation board manufactured by the Conwed Corporation. After each shot, an attempt was made to identify items which impacted on the backstop and rebounded without penetration. The fragment damage is shown in Figure 33. After the shots, the backstops were returned to the laboratory, where the fragments were recovered and weighed. The penetration, angle of entry, and area of entry were measured. Typical fragments are shown in Figures 34 and 35. The velocities of the fragments are presented in Table 8.

Results of High-Speed Camera Coverage

Before each shot, a 10-foot distance was marked off at a distance to be in the area of interest, parallel to each film plane, and photographed to provide a distance calibration on the film. The timing signals recorded on the film gave the film speed and the time between frames. It was thus possible to determine the velocity of a fragment in the direction parallel to the film plane by noting the displacement of the fragment on successive frames.

---

* Johns Hopkins University. Ballistics Analysis Laboratory. Report BAL-TR-61: The calibration of wallboard for the determination of particle speed, by D. Malick. Baltimore, Md., May 1966. (AD 485059)

The location of the fragment on the film was tracked and measured periodically with a Vangard motion analyzer. This device provides an automatic readout of X and Y position of a pointer moving across the projected film image. The absolute velocity of a fragment was then determined by combining the component velocities measured from two cameras acting at different angles. A summary of the component velocity data is given in Table 9. Unfortunately, the number of fragments visible from more than one angle was very limited. The following items were identified from more than one camera:

Item	Velocity (fps)	Weight (lb)
Pivot, part A	51	34.0
Piece flywheel housing, part P	58	7.3
Square metal piece	37	–
Clutch plate, part H2	29	15.0

Of these, the only item which struck the backstops was the piece of the flywheel housing. The backstop indicated the velocity to be 53 fps, which compares favorably with the 58 fps from the cameras. Further recovery of data was hindered by a malfunction of one of the cameras and the obscuring of fragments by the flame and smoke of the blast. Typical frames are shown in Figure 36.

The angle and field of coverage viewed by camera A was perpendicular to many of the fragments seen. The velocity components determined from these fragments are probably close to the actual velocity. The actual velocities, if they could be determined from cameras B and C, probably would not exceed the component velocities by 25%.

Discussion of Velocity Data

It was observed that the blast broke and shattered most of the items—including items composed of 1-inch-thick cast iron. There was evidence on many pieces of high-temperature (2,000°F) melting of the metal and local high-velocity impact damage of colliding fragments. The extent of damage and machine part breakup depends on the type of material, size and location of the part, and the amount of confinement. Cast items showed much more severe breakup than did wrought alloys, as would be expected. Chain was observed to break up and significantly increased the number of small high-velocity fragments. The confinement produced by the machine parts surrounding the explosive rounds reduced the spread of primary fragments from the casing of the round.

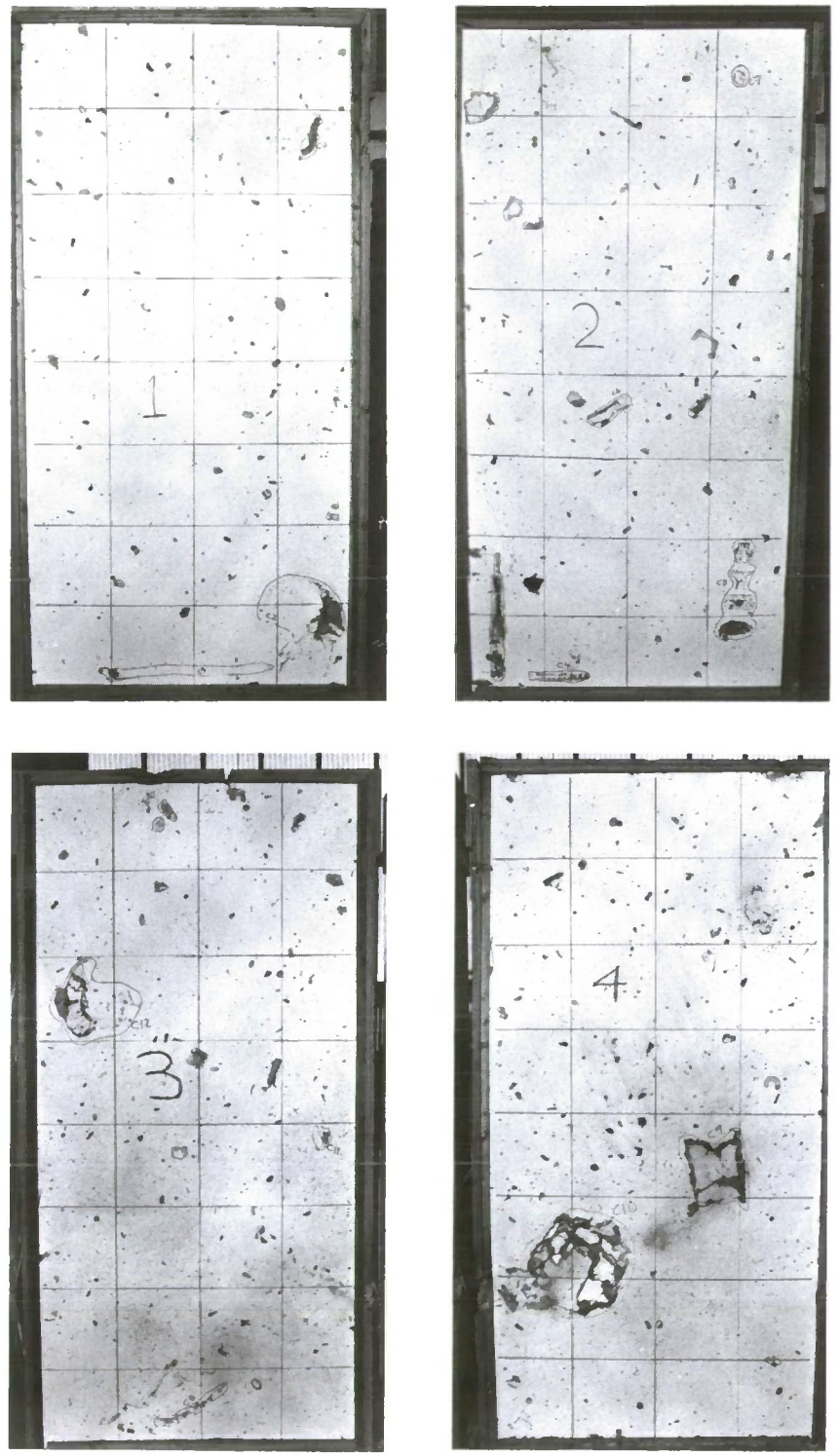

Figure 33. Postshot view of backstops, showing impact of fragments.

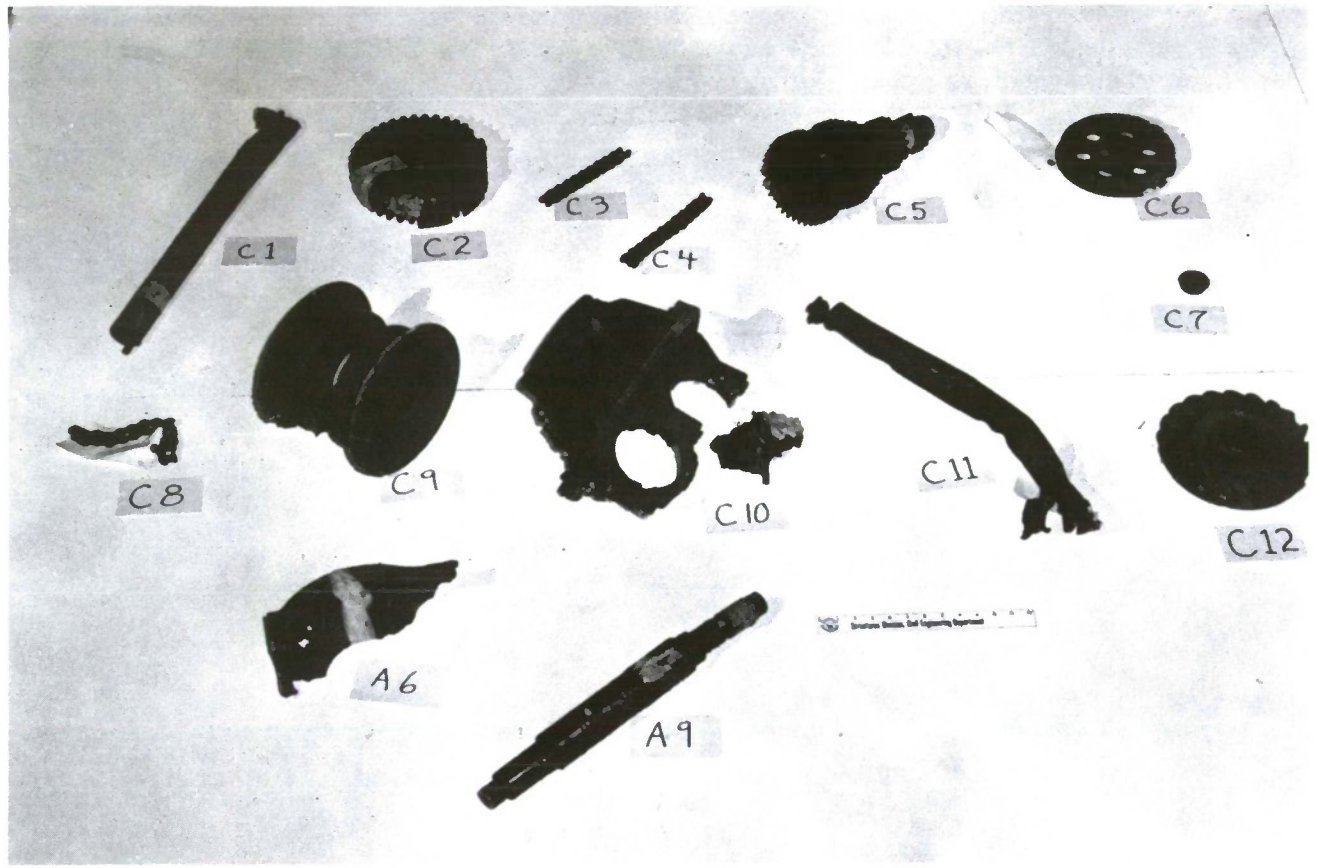

Figure 34. Large fragments that struck backstops.

Figure 35. Small fragments that struck backstops.

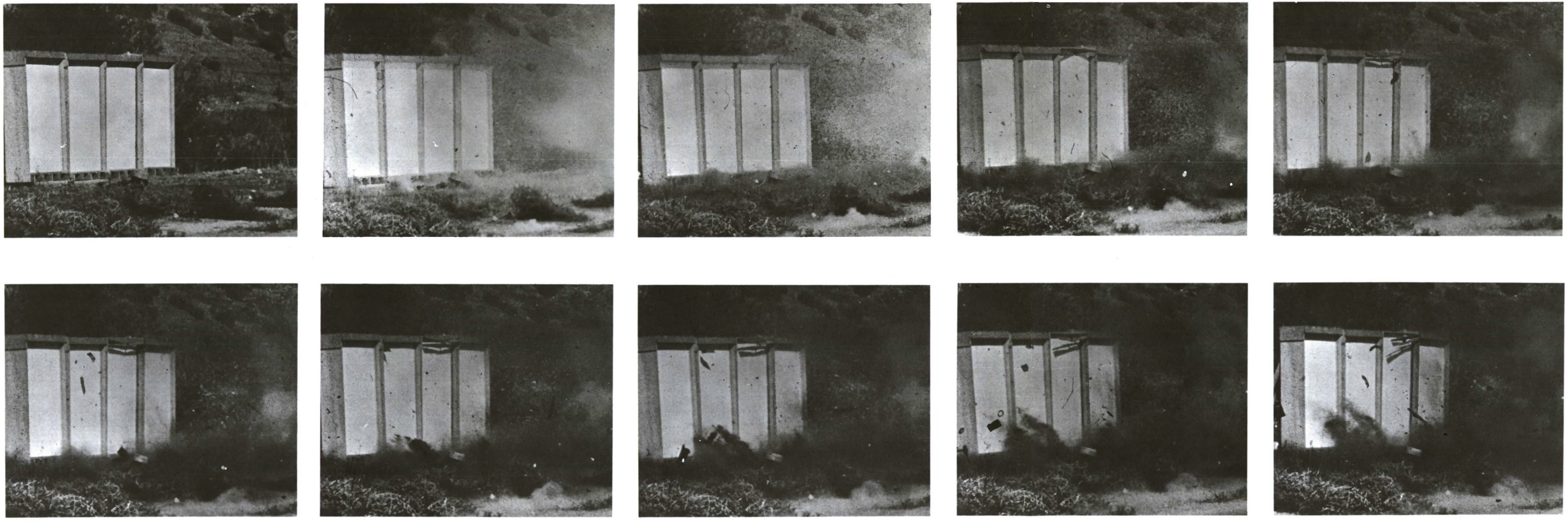

Note: Total coverage ≈ 0.65 sec.

Figure 36. High-speed photographs of fragments.

Table 8a. Velocity of Fragments Striking Backstop 1

Penetration (in.)	Weight (lb)	Area (sq in.)	Entry Angle (rad)	Velocity (fps)	Remarks
0.125	6.410	15.300	0.000	10	C1. Conveyor table roller.
0.500	24.000	34.900	0.000	20	C2. Steel gear, part F.
0.500	0.150	0.650	0.000	63	
0.500	0.011	0.300	0.000	365	
0.500	0.010	0.250	0.000	339	
0.500	0.010	0.350	0.000	460	
0.500	0.019	0.400	0.000	284	
0.500	0.019	0.500	0.000	348	
0.500	0.025	0.550	0.000	293	
0.500	0.010	0.041	0.000	65	
1.000	0.550	3.920	0.000	167	C3. Chain.
1.000	0.023	0.350	0.000	368	
1.000	0.025	0.650	0.000	598	
1.000	0.023	0.600	0.000	601	
1.000	0.010	0.350	0.000	806	
1.000	0.021	1.350	0.000	1,368	
1.000	0.010	0.200	0.000	485	
1.000	0.023	0.600	0.000	601	
1.000	0.011	0.320	0.000	679	
1.000	0.016	0.450	0.000	651	
1.500	0.020	0.300	0.000	507	
1.500	0.010	0.200	0.000	673	
1.500	0.012	0.500	0.000	1,304	
1.500	0.012	0.260	0.000	720	
1.500	0.018	0.800	0.000	1,365	
1.500	0.010	0.600	0.000	1,826	
2.000	0.010	0.150	0.000	654	
2.500	0.019	0.290	0.000	781	
4.000	0.008	0.250	0.524	2,431	Primary fragment.
5.000	0.025	1.050	0.000	3,401	Primary fragment.
7.500	0.020	0.780	0.000	4,445	Primary fragment.

Table 8b. Velocity of Fragments Striking Backstop 2

Penetration (in.)	Weight (lb)	Area (sq in.)	Entry Angle (rad)	Velocity (fps)	Remarks
0.250	0.010	0.380	0.000	283	Piece of chain.
0.250	0.100	0.450	0.000	37	
0.250	0.005	0.290	0.000	424	
0.500	16.000	35.400	0.000	29	Short shaft, part T.
0.500	0.100	5.900	0.000	688	Piece of metal.
0.500	0.020	0.084	0.000	65	Piece of chain.
0.500	0.010	0.300	0.000	400	
0.500	0.018	0.400	0.000	299	
0.500	0.012	0.400	0.000	437	
0.500	0.012	0.450	0.000	487	
0.063	0.020	0.650	0.000	78	Piece of chain.
1.000	0.370	3.400	0.000	214	C7. Piece of conveyor table.
1.000	34.500	40.520	0.000	28	C5. Gear from transmission, part Z.
1.000	0.630	10.050	0.000	347	C4. Chain.
1.000	12.000	10.050	0.000	21	C6. Cast wheel, part E3.
1.000	0.030	0.035	0.000	35	Piece of chain.
1.000	0.010	0.600	0.000	1,315	
1.000	0.010	0.350	0.000	806	
1.000	0.015	0.330	0.000	522	
1.000	0.150	0.300	0.000	55	
1.000	0.015	0.300	0.000	479	
1.500	7.330	11.200	0.000	53	Piece of flywheel, part P.
1.500	0.010	0.170	0.000	581	
2.000	0.012	0.400	0.698	1,552	
2.500	0.017	0.330	0.524	1,053	
5.500	0.007	0.370	0.000	4,708	Primary fragment.
6.500	0.001	0.100	0.175	10,298	Primary fragment.
7.000	0.005	0.300	0.436	6,843	Primary fragment.
7.500	0.007	0.600	0.175	9,464	

Table 8c. Velocity of Fragments Striking Backstop 3

Penetration (in.)	Weight (lb)	Area (sq in.)	Entry Angle (rad)	Velocity (fps)	Remarks
0.250	0.348	1.650	0.000	38	Bolt.
0.500	22.000	39.130	0.000	24	C12.
0.500	0.760	8.820	0.000	147	C8. Chain.
0.500	0.046	0.660	0.000	195	
0.500	0.009	0.100	0.000	162	
0.500	0.019	0.190	0.000	144	
0.500	0.020	0.200	0.000	144	
0.500	0.008	0.200	0.000	341	
0.500	0.255	1.850	0.000	99	Bolt.
1.000	6.590	1.950	0.000	8	C11. Conveyor table roller.
1.000	0.009	0.250	0.000	655	
1.000	0.006	0.300	0.000	1,132	
1.000	0.026	0.590	0.000	528	
1.000	0.011	0.630	0.000	1,257	
1.000	0.013	0.200	0.000	379	
1.000	0.003	0.100	0.000	800	
1.000	0.003	0.100	0.000	800	
1.000	0.008	0.270	0.000	785	
1.500	0.015	0.200	0.000	460	
1.500	0.014	0.500	0.000	1,128	
1.500	0.011	0.300	0.000	890	
1.500	0.002	0.050	0.000	867	
1.000	0.002	0.050	0.000	624	
2.000	0.004	0.200	0.000	2,009	
2.500	0.030	0.410	0.000	696	
2.500	0.008	0.200	0.000	1,255	
3.000	0.011	0.400	0.000	2,024	
3.000	0.015	0.230	0.000	915	
3.000	0.004	0.150	0.000	2,148	
4.000	0.002	0.080	0.000	2,937	
4.500	0.002	0.030	0.000	1,326	
8.000	0.005	0.550	0.000	12,532	Primary fragment.

Table 8d. Velocity of Fragments Striking Backstop 4

Penetration (in.)	Weight (lb)	Area (sq in.)	Entry Angle (rad)	Velocity (fps)	Remarks
0.125	0.026	0.850	0.000	136	
0.500	0.013	0.430	0.000	433	
0.500	0.004	0.380	0.000	1,172	
0.500	0.011	0.230	0.000	287	
0.500	0.013	0.600	0.000	586	
0.500	0.015	0.250	0.000	231	
1.000	0.013	0.500	0.000	871	
1.000	0.011	0.200	0.000	443	
1.000	0.002	0.070	0.000	847	
1.000	0.006	0.230	0.000	889	
1.000	0.006	0.100	0.000	417	
1.500	0.255	1.500	0.000	200	Bolt.
2.000	0.002	0.110	0.785	2,701	
2.500	44.000	64.000	0.000	72	C9. Steel wheel, part L.
3.000	42.000	132.000	0.000	169	C10. Rear-end housing, part O.
5.000	0.002	0.100	0.000	4,308	Primary fragment.
5.000	0.004	0.380	0.000	7,552	Primary fragment.
6.500	0.006	0.330	0.000	5,615	Primary fragment.
10.000	0.008	0.250	0.000	4,720	Primary fragment.
10.000	0.006	0.200	0.000	5,050	Primary fragment.
10.000	0.004	0.150	0.000	5,690	Primary fragment.
10.500	0.008	0.250	0.000	4,910	Primary fragment.

Table 9. Fragment Velocity Determined From High-Speed Cameras

Fragment	Velocity (fps)	Elevation Angle (deg)[a]	Remarks
Camera A, Shot 1			
A1-1	171	16	
A2-2	78	12	
A1-3	73	12	Piece, yellow flywheel, part P.
A1-4	47	2	Pivot, part A, weight 34 lb. (See B1-4.)
A1-5	35	9	Piece, yellow flywheel, part P.
A1-6	20	- 1	Piece, yellow flywheel.
A1-7	122	24	
A1-8	73	10	
A1-9	36	11	
A1-10	73	11	
Camera B, Shot 1			
B1-1	172	7	Metal piece.
B1-2	103	23	
B1-3	57	11	Piece, yellow flywheel, weight 7.33 lb. Struck backstop. (See A1-6, C1-2.)
B1-4	50	1	Pivot, part A, weight 34 lb. (See A1-4.)
B1-5	31	16	Square metal piece.
B1-6	29	- 9	Short shaft, weight 16 lb. Struck backstop.
B1-7	17	5	Piece, yellow flywheel, part P.
B1-8	14	-43	Transmission, part Z, weight 170 lb.
B1-9	12	-51	Top piece from transmission, part Z, weight 16 lb.
B1-10	18	- 8	Square metal piece. (See C1-4.)
B1-11	24	-18	Clutch plate, part H2, weight 15 lb. (See C1-3.)
B1-12	28	22	Metal piece.

continued

Table 9. Continued

Fragment	Velocity (fps)	Elevation Angle (deg)[a]	Remarks
Camera C, Shot 1			
C1-1	203	35	Metal.
C1-2	31	16	Piece, yellow flywheel, part P, weight 7.33 lb. Struck backstop. (See B1-3, A1-6.)
C1-3	25	2	Clutch plate, part H2, weight 15 lb. (See B1-11.)
C1-4	35	7	Square metal piece. (See B1-10.)
C1-5	24	2	Rear-end housing, part N, weight 67 lb.
C1-6	41	18	Piece clutch plate, part H2.
C1-7	60	6	Metal.
Camera A, Shot 2			
A2-1	76	16	Rear end, part N, weight 67 lb.
A2-2	44	4	
A2-3	121	26	
A2-4	132	24	
A2-5	44	14	
Camera C, Shot 2			
C2-1	85	- 2	Short shaft, part T, weight 16 lb.
C2-2	20	17	Conveyor table roller.
C2-3	140	38	
Camera A, Shot 3			
A3-1	47	- 1	
A3-2	180	13	
A3-3	80	26	
A3-4	41	- 3	
A3-5	222	20	

continued

Table 9. Continued

Fragment	Velocity (fps)	Elevation Angle (deg)[a]	Remarks
Camera A, Shot 3 (Continued)			
A3-6	116	5	
A3-7	54	- 7	
A3-8	89	10	Small rear-end housing, part O, weight 58 lb.
Camera C, Shot 3			
C3-1	77	51	Conveyor table roller.
C3-2	96	10	Ring.

[a] Degrees from horizontal.

A summary of velocity—weight data is presented in Figure 37 and tabulated below:

Weight (lb)	Average Velocity (fps)	Upper Limit Velocity (fps)
Over 10	50	100
1.0 to 10	100	200
0.1 to 1.0	150	500
0.01 to 0.1	500	2,000
0.001 to 0.01	1,200	4,000

Most of the high-velocity items around 0.01 pound were pieces of chain. The data presented should be looked upon as giving orders of magnitude of fragment velocities rather than exact values. The velocity of the fragments will depend on the type, quantity, and arrangement of the machine parts.

SUMMARY OF RESULTS

Tests were conducted to evaluate the blast environment within the cubicle and on the surrounding structure. It was found that for a fully vented cubicle peak pressures on the surrounding structure were not significantly

affected by variations in the elevation of the charge. Multiple peaks were produced by shock wave reflections. The pressures resulting from the simultaneous detonation of three separate charges closely approximated that from a single charge of the same total weight. Negative pressures were observed to provide a lifting effect on the structure's roof and therefore should be considered as a factor in the design of the structure. With a fully vented cubicle the magnitude of the positive pressures on the roof was high enough to cause an inward collapse of a portion of the roof of the structure. The venting area of the cubicle was reduced and it was observed that the pressures on the roof could be brought within safe limits. The reduced venting resulted in a buildup of gas accumulation pressures within the cubicle, increasing the impulse on the walls of the cubicle.

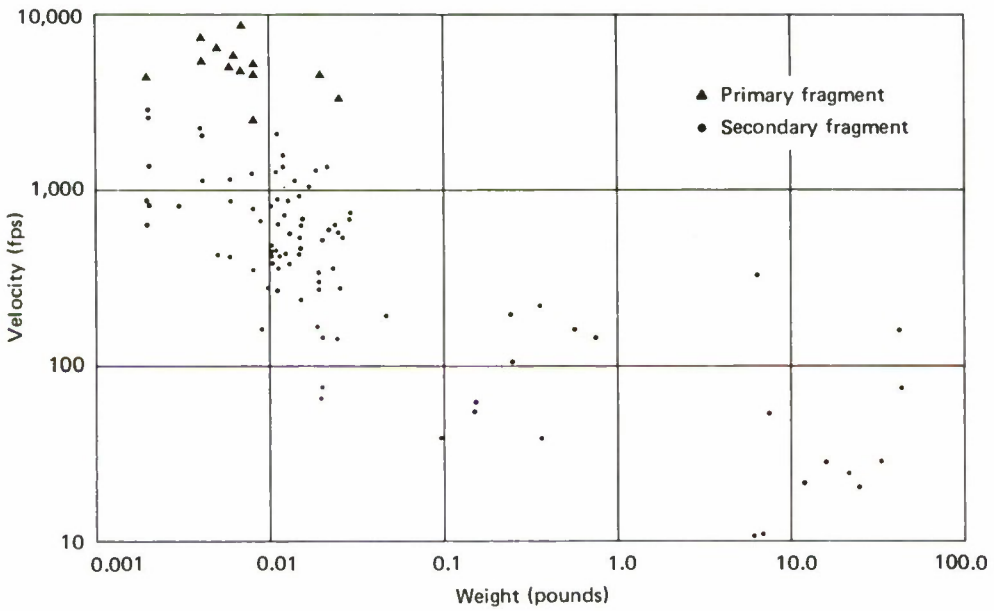

Figure 37. Fragment weight versus velocity for fragments collected in backstops.

The velocity and distribution of secondary fragments were determined by camera coverage and backstop penetration. Large heavy objects were thrown considerable distances; a steel gear weighing 34.5 pounds was thrown 219 feet. The velocity of many of the fragments was high enough to be hazardous.

ACKNOWLEDGMENTS

The blast environment tests were conducted at the Pacific Missile Range, Point Mugu, California. Mr. J. E. Tancreto, NCEL Research Structural Engineer, coordinated and assisted in several phases of the test program. Mr. D. H. Johnson, NCEL Instrumentation Engineer, and Mr. R. A. Giaimo, NCEL Instrumentation Technician, set up and operated the instrumentation. Explosives were set and detonated under the supervision of Mr. P. R. Smith of the Pacific Missile Range Operations Department, Launching Division. Data were digitized and plotted under the direction of Mr. L. W. Fuller at the Pacific Missile Range Data Center.

The 81-mm fragment velocity tests were conducted at the U.S. Marine Corps Base, Camp Pendleton, California. The tests were coordinated by the West Coast Test Branch, Marine Corps Tactical Systems Support Activity under the supervision of Major V. E. Hobbs, USMC, and Warrant Officer R. W. Porter, USMC. The author gratefully acknowledges the assistance of the above people.

DISTRIBUTION LIST

SNDL Code	No. of Activities	Total Copies	
—	1	12	Defense Documentation Center
FKAIC	1	3	Naval Facilities Engineering Command
FKNI	6	6	NAVFAC Engineering Field Divisions
FKN5	9	9	Public Works Centers
FA25	1	1	Public Works Center
—	9	9	RDT&E Liaison Officers at NAVFAC Engineering Field Divisions and Construction Battalion Centers
—	302	302	NCEL Special Distribution List No. 6 for Government activities interested in reports on Structural Control

Naval Civil Engineering Laboratory
DETERMINATION OF BLAST LEAKAGE PRESSURES AND FRAGMENT VELOCITY FOR FULLY VENTED AND PARTIALLY VENTED PROTECTIVE CUBICLES, by J. M. Ferritto
TR-780 56 p. illus November 1972 Unclassified
1. 8last pressures—full and partial venting 2. Secondary fragments I. 51-031

Blast leakage pressures acting on a structure surrounding a protective cubicle were experimentally determined in a one-third scale model test. Nineteen pressure transducers were used to record the blast environment within the cubicle and on the surrounding structure. Variations in venting area were tested. Results indicate that the pressures can be sufficiently high to cause damage to conventional construction; however, the pressures can be reduced to safe levels by restricting the venting. The velocity of secondary fragments produced from the breakup of simulated processing equipment subjected to the blast of full-size 81-mm mortars was determined. Photographic coverage and calculation of fragment penetration in backstops indicate heavy secondary fragments are capable of traveling considerable distances.

Naval Civil Engineering Laboratory
DETERMINATION OF BLAST LEAKAGE PRESSURES AND FRAGMENT VELOCITY FOR FULLY VENTED AND PARTIALLY VENTED PROTECTIVE CUBICLES, by J. M. Ferritto
TR-780 56 p. illus November 1972 Unclassified
1. Blast pressures—full and partial venting 2. Secondary fragments I. 51-031

Blast leakage pressures acting on a structure surrounding a protective cubicle were experimentally determined in a one-third scale model test. Nineteen pressure transducers were used to record the blast environment within the cubicle and on the surrounding structure. Variations in venting area were tested. Results indicate that the pressures can be sufficiently high to cause damage to conventional construction; however, the pressures can be reduced to safe levels by restricting the venting. The velocity of secondary fragments produced from the breakup of simulated processing equipment subjected to the blast of full-size 81-mm mortars was determined. Photographic coverage and calculation of fragment penetration in backstops indicate heavy secondary fragments are capable of traveling considerable distances.

Naval Civil Engineering Laboratory
DETERMINATION OF BLAST LEAKAGE PRESSURES AND FRAGMENT VELOCITY FOR FULLY VENTED AND PARTIALLY VENTED PROTECTIVE CUBICLES, by J. M. Ferritto
TR-780 56 p. illus November 1972 Unclassified
1. Blast pressures—full and partial venting 2. Secondary fragments I. 51-031

Blast leakage pressures acting on a structure surrounding a protective cubicle were experimentally determined in a one-third scale model test. Nineteen pressure transducers were used to record the blast environment within the cubicle and on the surrounding structure. Variations in venting area were tested. Results indicate that the pressures can be sufficiently high to cause damage to conventional construction; however, the pressures can be reduced to safe levels by restricting the venting. The velocity of secondary fragments produced from the breakup of simulated processing equipment subjected to the blast of full-size 81-mm mortars was determined. Photographic coverage and calculation of fragment penetration in backstops indicate heavy secondary fragments are capable of traveling considerable distances.

Naval Civil Engineering Laboratory
DETERMINATION OF BLAST LEAKAGE PRESSURES AND FRAGMENT VELOCITY FOR FULLY VENTED AND PARTIALLY VENTED PROTECTIVE CUBICLES, by J. M. Ferritto
TR-780 56 p. illus November 1972 Unclassified
1. Blast pressures—full and partial venting 2. Secondary fragments I. 51-031

Blast leakage pressures acting on a structure surrounding a protective cubicle were experimentally determined in a one-third scale model test. Nineteen pressure transducers were used to record the blast environment within the cubicle and on the surrounding structure. Variations in venting area were tested. Results indicate that the pressures can be sufficiently high to cause damage to conventional construction; however, the pressures can be reduced to safe levels by restricting the venting. The velocity of secondary fragments produced from the breakup of simulated processing equipment subjected to the blast of full-size 81-mm mortars was determined. Photographic coverage and calculation of fragment penetration in backstops indicate heavy secondary fragments are capable of traveling considerable distances.

Naval Civil Engineering Laboratory
DETERMINATION OF BLAST LEAKAGE PRESSURES AND FRAGMENT VELOCITY FOR FULLY VENTED AND PARTIALLY VENTED PROTECTIVE CUBICLES, by J. M. Ferritto
TR-780 56 p. illus November 1972 Unclassified
1. Blast pressures—full and partial venting 2. Secondary fragments I. 51-031

Blast leakage pressures acting on a structure surrounding a protective cubicle were experimentally determined in a one-third scale model test. Nineteen pressure transducers were used to record the blast environment within the cubicle and on the surrounding structure. Variations in venting area were tested. Results indicate that the pressures can be sufficiently high to cause damage to conventional construction; however, the pressures can be reduced to safe levels by restricting the venting. The velocity of secondary fragments produced from the breakup of simulated processing equipment subjected to the blast of full-size 81-mm mortars was determined. Photographic coverage and calculation of fragment penetration in backstops indicate heavy secondary fragments are capable of traveling considerable distances.

Naval Civil Engineering Laboratory
DETERMINATION OF BLAST LEAKAGE PRESSURES AND FRAGMENT VELOCITY FOR FULLY VENTED AND PARTIALLY VENTED PROTECTIVE CUBICLES, by J. M. Ferritto
TR-780 56 p. illus November 1972 Unclassified
1. Blast pressures—full and partial venting 2. Secondary fragments I. 51-031

Blast leakage pressures acting on a structure surrounding a protective cubicle were experimentally determined in a one-third scale model test. Nineteen pressure transducers were used to record the blast environment within the cubicle and on the surrounding structure. Variations in venting area were tested. Results indicate that the pressures can be sufficiently high to cause damage to conventional construction; however, the pressures can be reduced to safe levels by restricting the venting. The velocity of secondary fragments produced from the breakup of simulated processing equipment subjected to the blast of full-size B1-mm mortars was determined. Photographic coverage and calculation of fragment penetration in backstops indicate heavy secondary fragments are capable of traveling considerable distances.

Naval Civil Engineering Laboratory
DETERMINATION OF BLAST LEAKAGE PRESSURES AND FRAGMENT VELOCITY FOR FULLY VENTED AND PARTIALLY VENTED PROTECTIVE CUBICLES, by J. M. Ferritto
TR-7B0 56 p. illus November 1972 Unclassified
1. Blast pressures—full and partial venting 2. Secondary fragments I. 51-031

Blast leakage pressures acting on a structure surrounding a protective cubicle were experimentally determined in a one-third scale model test. Nineteen pressure transducers were used to record the blast environment within the cubicle and on the surrounding structure. Variations in venting area were tested. Results indicate that the pressures can be sufficiently high to cause damage to conventional construction; however, the pressures can be reduced to safe levels by restricting the venting. The velocity of secondary fragments produced from the breakup of simulated processing equipment subjected to the blast of full-size 81-mm mortars was determined. Photographic coverage and calculation of fragment penetration in backstops indicate heavy secondary fragments are capable of traveling considerable distances.

Naval Civil Engineering Laboratory
DETERMINATION OF BLAST LEAKAGE PRESSURES AND FRAGMENT VELOCITY FOR FULLY VENTED AND PARTIALLY VENTED PROTECTIVE CUBICLES, by J. M. Ferritto
TR-7B0 56 p. illus November 1972 Unclassified
1. Blast pressures—full and partial venting 2. Secondary fragments I. 51-031

Blast leakage pressures acting on a structure surrounding a protective cubicle were experimentally determined in a one-third scale model test. Nineteen pressure transducers were used to record the blast environment within the cubicle and on the surrounding structure. Variations in venting area were tested. Results indicate that the pressures can be sufficiently high to cause damage to conventional construction; however, the pressures can be reduced to safe levels by restricting the venting. The velocity of secondary fragments produced from the breakup of simulated processing equipment subjected to the blast of full-size B1-mm mortars was determined. Photographic coverage and calculation of fragment penetration in backstops indicate heavy secondary fragments are capable of traveling considerable distances.

Unclassified

Security Classification

DOCUMENT CONTROL DATA - R & D

(Security classification of title, body of abstract and indexing annotation must be entered when the overall report is classified)

1. ORIGINATING ACTIVITY (Corporate author)	2a. REPORT SECURITY CLASSIFICATION
Naval Civil Engineering Laboratory Port Hueneme, California 93043	Unclassified
	2b. GROUP

3. REPORT TITLE

DETERMINATION OF BLAST LEAKAGE PRESSURES AND FRAGMENT VELOCITY FOR FULLY VENTED AND PARTIALLY VENTED PROTECTIVE CUBICLES

4. DESCRIPTIVE NOTES (Type of report and inclusive dates)

Not final; October 1971 – January 1972

5. AUTHOR(S) (First name, middle initial, last name)

J. M. Ferritto

6. REPORT DATE	7a. TOTAL NO. OF PAGES	7b. NO. OF REFS
November 1972	56	2

8a. CONTRACT OR GRANT NO.	9a. ORIGINATOR'S REPORT NUMBER(S)
b. PROJECT NO. 51-031	TR-780
c.	9b. OTHER REPORT NO(S) (Any other numbers that may be assigned this report)
d.	

10. DISTRIBUTION STATEMENT

Distribution limited to U. S. Government agencies only; Test and Evaluation; November 1972. Other requests for this document must be referred to the Naval Civil Engineering Laboratory.

11. SUPPLEMENTARY NOTES	12. SPONSORING MILITARY ACTIVITY
	Picatinny Arsenal Dover, New Jersey 07801

13. ABSTRACT

Blast leakage pressures acting on a structure surrounding a protective cubicle were experimentally determined in a one-third scale model test. Nineteen pressure transducers were used to record the blast environment within the cubicle and on the surrounding structure. Variations in venting area were tested. Results indicate that the pressures can be sufficiently high to cause damage to conventional construction; however, the pressures can be reduced to safe levels by restricting the venting. The velocity of secondary fragments produced from the breakup of simulated processing equipment subjected to the blast of full-size 81-mm mortars was determined. Photographic coverage and calculation of fragment penetration in backstops indicate heavy secondary fragments are capable of traveling considerable distances.

DD FORM 1 NOV 65 1473 (PAGE 1)

S/N 0101-807-6801

Unclassified

Security Classification

14 KEY WORDS	LINK A		LINK B		LINK C	
	ROLE	WT	ROLE	WT	ROLE	WT
Protective cubicles						
Blast leakage pressures						
Fragment velocity						
Secondary fragments						
Explosion enclosure						
Personnel protection						
Vented cubicles						
Partially vented cubicles						
Pressure instrumentation measurements						
Scale modeling						
Gas pressure						